Cell Transplantation
Volume 31: 1–25

DOI: 10.1177/09636897221104451
journals.sagepub.com/home/cll
SAGE

Biocompatibility of Human Induced Pluripotent Stem Cell–Derived Retinal Progenitor Cell Grafts in Immunocompromised Rats

Ian C. Han[1,2], Laura R. Bohrer[1,2], Katherine N. Gibson-Corley[3], Luke A. Wiley[1,2], Arwin Shrestha[1,2], Brynnon E. Harman[1,2], Chunhua Jiao[1,2], Elliott H. Sohn[1,2], Rion Wendland[1,4], Brittany N. Allen[1,4], Kristan S. Worthington[1,4], Robert F. Mullins[1,2], Edwin M. Stone[1,2], and Budd A. Tucker[1,2]

Abstract

Loss of photoreceptor cells is a primary feature of inherited retinal degenerative disorders including age-related macular degeneration and retinitis pigmentosa. To restore vision in affected patients, photoreceptor cell replacement will be required. The ideal donor cells for this application are induced pluripotent stem cells (iPSCs) because they can be derived from and transplanted into the same patient obviating the need for long-term immunosuppression. A major limitation for retinal cell replacement therapy is donor cell loss associated with simple methods of cell delivery such as subretinal injections of bolus cell suspensions. Transplantation with supportive biomaterials can help maintain cellular integrity, increase cell survival, and encourage proper cellular alignment and improve integration with the host retina. Using a pig model of retinal degeneration, we recently demonstrated that polycaprolactone (PCL) scaffolds fabricated with two photon lithography have excellent local and systemic tolerability. In this study, we describe rapid photopolymerization-mediated production of PCL-based bioabsorbable scaffolds, a technique for loading iPSC-derived retinal progenitor cells onto the scaffold, methods of surgical transplantation in an immunocompromised rat model and tolerability of the subretinal grafts at 1, 3, and 6 months of follow-up ($n = 150$). We observed no local or systemic toxicity, nor did we observe any tumor formation despite extensive clinical evaluation, clinical chemistry, hematology, gross tissue examination and detailed histopathology. Demonstrating the local and systemic compatibility of biodegradable scaffolds carrying human iPSC-derived retinal progenitor cells is an important step toward clinical safety trials of this approach in humans.

Keywords

systemic toxicity, autologous cell replacement, subretinal transplantation, iPSC-derived retinal cell graft, human retinal engineering

Introduction

Loss of photoreceptor cells is a pathophysiologic feature shared between the common condition age-related macular degeneration and much rarer Mendelian retinal degenerative disorders, such as retinitis pigmentosa, Stargardt disease, and Usher syndrome. Unlike lower vertebrates (eg, salamander), which can rebuild their entire retina via activation of an endogenous progenitor cell population[1], the human retina has little intrinsic ability to regenerate following injury. The most promising treatment strategy for restoring vision to patients blinded by one of these disorders is stem cell-mediated photoreceptor cell replacement[2–16]. Unlike stem

[1] Institute for Vision Research, University of Iowa, Iowa City, IA, USA
[2] Department of Ophthalmology and Visual Sciences, Carver College of Medicine, University of Iowa, Iowa City, IA, USA
[3] Department of Microbiology & Immunology, Vanderbilt University Medical Center, Nashville, TN, USA
[4] Department of Biomedical Engineering, College of Engineering, University of Iowa, Iowa City, IA, USA

Submitted: November 22, 2021. Revised: March 30, 2022. Accepted: May 16, 2022.

Corresponding Author:
Budd A. Tucker, Institute for Vision Research, Department of Ophthalmology and Visual Science, Carver College of Medicine, University of Iowa, 375 Newton Road, Iowa City, IA 52242, USA.
Email: budd-tucker@uiowa.edu

cell-derived retinal pigmented epithelial (RPE) cells, which have been successfully transplanted in a number of human clinical trials[17–22], photoreceptor cells are light-detecting neurons that must extend their axons into the host retina and form synaptic connections with host bipolar cells to restore visual function.

A variety of different donor cell types have been evaluated for retinal cell transplantation[23,24]. For example, fate-restricted retinal progenitor and photoreceptor precursor cells can be obtained from fetal donors and transplanted directly into patients[25–29]. These cell types have been shown to be at a developmental stage that is suitable for photoreceptor cell replacement, but their fetal origin is associated with significant practical and ethical limitations. In contrast to these immediately transplantable fetal cells, embryonic and induced pluripotent stem cells both require many weeks of *in vitro* differentiation prior to transplantation. However, the latter cell types both have the tremendous advantage of unlimited self-renewal and have become the strategy of choice for cell replacement. Patient-derived induced pluripotent stem cells (iPSCs) have the additional advantage that they can be derived from and transplanted into the same patient, thus creating an immunologic match, and avoiding the need for lifelong immunosuppression.

Although several studies have illustrated the potential for stem cell-derived photoreceptor cell replacement to restore vision[7,13,30–33], a major limitation to this therapeutic application has been the loss of donor cells following subretinal delivery. For instance, up to 95% of cells delivered as a subretinal bolus cell suspension are lost through a combination of efflux from the injection site and apoptosis triggered by the loss of adhesion and the shear stresses that occur during dissociation of mature cell cultures and injection through small-bore cannulas[34–36]. To overcome these limitations, we and others have explored the use of biodegradable polymers as cell support scaffolds[34–42]. These scaffolds are designed to provide donor cells with the structural support required to prevent efflux and mitigate apoptosis[34–42]. In addition, scaffolds can be designed to promote proper photoreceptor cell alignment, packing density, maturation and synaptic integration following transplantation[37,38,41,42].

We recently evaluated local and systemic biocompatibility of a polycaprolactone (PCL) cell support scaffold following subretinal transplantation in a pig model of advanced retinal degeneration[37]. In addition to demonstrating that PCL scaffolds and their degradation products are well tolerated, we confirmed that the subretinal transplantation strategy and instrumentation that will be used clinically were both safe and effective. That is, we were able to successfully place and maintain 3D scaffolds in the subretinal space of a pig model of advanced retinitis pigmentosa without serious adverse events. The next step toward developing a clinical autologous photoreceptor cell replacement strategy is to demonstrate that PCL-supported patient-derived retinal progenitor cells (ie, retinal cell grafts) are non-tumorigenic and do not induce local or systemic toxicity following subretinal transplantation. In choosing a recipient model system for these experiments we had two main considerations: (1) the host should be immunocompromised and in turn conducive to receiving a xenograft, and (2) the host should have eyes large enough to have a 3D retinal cell graft placed in the subretinal space and yet small enough to be housed in large numbers for an extended period of time. The latter feature is essential for one to be able to test grafts generated from multiple different patients for up to 6 months following placement. The Rowett Nude rats (RNU) rat is a readily available immunocompromised animal that at just 2 months of age has eyes large enough to receive a 1-mm subretinal graft of the same thickness intended for human clinical use. In addition, the baseline health status, which includes hematology and clinical chemistry parameters as well as strain specific lesions, has been thoroughly documented[43–47]. While this animal is not suitable for evaluating treatment efficacy (ie, it does not suffer from an inherited retinal degeneration), the above features make it ideally suited for use in the local and systemic toxicity studies reported later in this article.

In this study, we describe fabrication of a retinal cell graft (DTVRF-hiPSC-ARG), methods for subretinal transplantation in an immunodeficient RNU rat model, as well as comprehensive local and systemic tolerability analyses following subretinal delivery with 1, 3, and 6 months of follow-up. We demonstrate that DTVRF-hiPSC-ARGs do not induce tumor formation or cause local or systemic toxicity following subretinal transplantation.

Materials and Methods

Ethics Statement

Approval to obtain dermal fibroblast cells and generate iPSCs from patients with inherited retinal degeneration and normal controls was obtained under informed consent. This study was reviewed and approved by the University of Iowa Institutional Review Board (IRB# 200202022). All rat experiments were conducted with the approval of the University of Iowa Animal Care and Use Committee (animal welfare assurance #8051317) and were consistent with the ARVO Statement for the Use of Animals in Ophthalmic and Vision Research.

Fabrication of PCL Retinal Progenitor Cell Delivery Scaffolds

PCL-acrylate was fabricated by Creative PEGWorks as follows: PCL triol (M_n ~300 g/mol) was functionalized by mixing it with potassium carbonate and acryloyl chloride at a 1:3:3 ratio. The PCL triol was dissolved in methylene chloride (1:2 v/v) and then mixed with potassium carbonate. Acryloyl chloride was added dropwise to the PCL triol-potassium carbonate mixture. The reaction mixture was

filtered to remove solids. Sodium bicarbonate was added to the mixture at a 1:1 ratio and run through a separatory funnel. Excess solvent was removed from the functionalized PCL by rotary evaporation and the final product stored in dry, airtight containers at −20°C. The degree of functionalization and final molecular weight were measured for each batch using nuclear magnetic resonance (^{1}H NMR) and gel permeation chromatography, respectively. One gram of functionalized PCL (Creative PEGWorks, Chapel Hill, NC, USA; Cat#: PCL-AC-300-50g) and 100 µl of photoinitiator solution (0.1 g Irgacure® 2959 in 1 ml of sterile ethanol, Advanced BioMatrix, Inc., Carlsbad, CA, USA) were combined and used for polymerization.

Retinal progenitor cell scaffolds were generated via photopolymerization using UV light (approximately 100 lumens/cm^2) and a photomask containing 75 µm black spots spaced at 25 µm in a hexagonal pattern. Following fabrication, scaffolds were removed from the polymerization chamber and placed onto a 6-well Millicell insert (EMD Millipore; Cat#: MCMP06H48, Burlington, MA, USA) where a vacuum allowed active rinsing of the scaffolds. The scaffold was rinsed 10 times with 1 ml of sterile phosphate buffer saline (PBS) (Gibco/Thermo Fisher Scientific, Waltham, MA, USA) and then submerged in sterile PBS overnight. Following the final rinse, scaffolds were placed into a 12-well plate, submerged in sterile PBS, and double packaged in an instant sealing sterilization pouch to be terminally sterilized via gamma irradiation. The scaffolds remained in the sealed sterilization pouch until ready for use, at which time they were opened in a laminar flow hood to maintain aseptic processing. Scaffolds were fabricated 2 to 3 weeks prior to being seeded.

Generation and Differentiation of Patient-Derived iPSCs

In this study, four independent iPSC lines [a normal control and three patients (P1 and P2 were diagnosed with wolfram syndrome [ie, WFS1-associated disease affects retinal ganglion cells and patients retain normal photoreceptor cells throughout their life] and P3 was diagnosed with enhanced S cone syndrome [non-progressive disease in which the patient has an abundance of blue cones and few rod cells])] were generated and differentiated into transplantable retinal progenitor cells using our previously published protocols[48,49]. Briefly, each iPSC line was generated via reprogramming of dermal fibroblast using the CytoTune 2 Sendai viral reprogramming kit (Gibco/Thermo Fisher Scientific, Waltham, MA, USA). Following clonal expansion, karyotyping and scorecard analysis at passage 10, iPSCs were differentiated into 3D retinal organoids[48]. At 70 ± 5 days, retinal organoids were harvested, dissociated into individual retinal progenitor cells, and plated onto PCL scaffolds fabricated and sterilized as described above at a density of 40,000 cells per 1-mm circular graft (0.79 mm^2). From this point forward, DTVRF-hiPSC-ARG refers to these PCL scaffolds seeded with human iPSC-derived retinal progenitor cells. For immunocytochemistry, grafts were fixed with 4% paraformaldehyde and stained with the following primary antibodies overnight: OTX2 (R&D Systems; Cat#: AF1979, Minneapolis, MN, USA), Recoverin (EMD Millipore; Cat#: AB5585, Burlington, MA, USA), SOX2 (R&D Systems; Cat#: MAB2018), NRL (R&D Systems; Cat#: AF2945), NRL (R&D Systems; Cat#: AF2945), ARR3 (Lifespan Biosciences; Cat#: LS-C368677, Seattle, WA, USA), NR2E3 (R&D Systems; Cat#: PP-H7223-00), Opsin, red/green (EMD Millipore; Cat#: AB5405), Rhodopsin (EMD Millipore; Cat#: MAB5316). The following secondary antibodies (Thermo Fisher Scientific, Waltham, MA, USA) were incubated for 1 hour: donkey anti-goat 488 (Thermo Fisher Scientific; Cat#: A11055, Waltham, MA, USA), and donkey anti-rabbit 488 (Thermo Fisher Scientific; Cat#: R37118, Waltham, MA, USA), donkey anti-mouse 488 (Cat#: A21202), donkey anti-sheep 647 (Cat#: A21448), donkey anit-rabbit 647 (Cat#: A31573), donkey anti-goat 647 (Cat#: A21447). Cell nuclei were counterstained using DAPI (Thermo Fisher Scientific; Cat#: 62248) or SYTOX Orange (Thermo Fisher Scientific; Cat#: S11368, Waltham, MA, USA).

Subretinal Transplantation and Study Design

To assess both local and systemic tolerability of DTVRF-hiPSC-ARG, T-cell deficient homozygous Rowett Nude rats (RNU-/-; Cr:NIH-RNU; Charles River, Wilmington, MA, USA, hereafter referred to as RNU) were utilized. Rats were anesthetized with isoflurane and eyes were dilated with 1–2 drops of 1% tropicamide (Alcon Laboratories, Fort Worth, TX, USA). All rat surgeries were performed by a fellowship-trained retina surgeon (I.C.H.). Under an operating microscope (Leica M620; Leica Microsystems, Inc., Wetzlar, Germany), subretinal transplantation of grafts was performed using a modified version of previously described methods[50,51]. In brief, a limited conjunctival peritomy was created to expose the temporal sclera (Fig. 1A). A 15° sideport blade (Beckon Dickinson and Company, Waltham, MA, USA) was used to create a transscleral, transretinal incision into the vitreous cavity (Fig. 1B). Any prolapsed vitreous was trimmed with Vannas scissors and balanced salt solution was then dripped into the incision site with a 30-gauge anterior chamber cannula (Beaver-Visitec International, Waltham, MA, USA) to create a localized retinal detachment (Fig. 1C). Grafts were transported to the surgical suite in a 40-µm cell strainer contained within a 6-well culture plate (Corning Incorporated, Corning, NY, USA) (Fig. 1D) containing 1× Hanks' Balanced Salt solution (Thermo Fischer Scientific, Waltham, MA, USA). Each individual graft was elevated from the transport solution using the strainer and grasped at its edge with McPherson tying forceps (Miltex Inc., York, PA, USA), which were then used to transplant the polymer

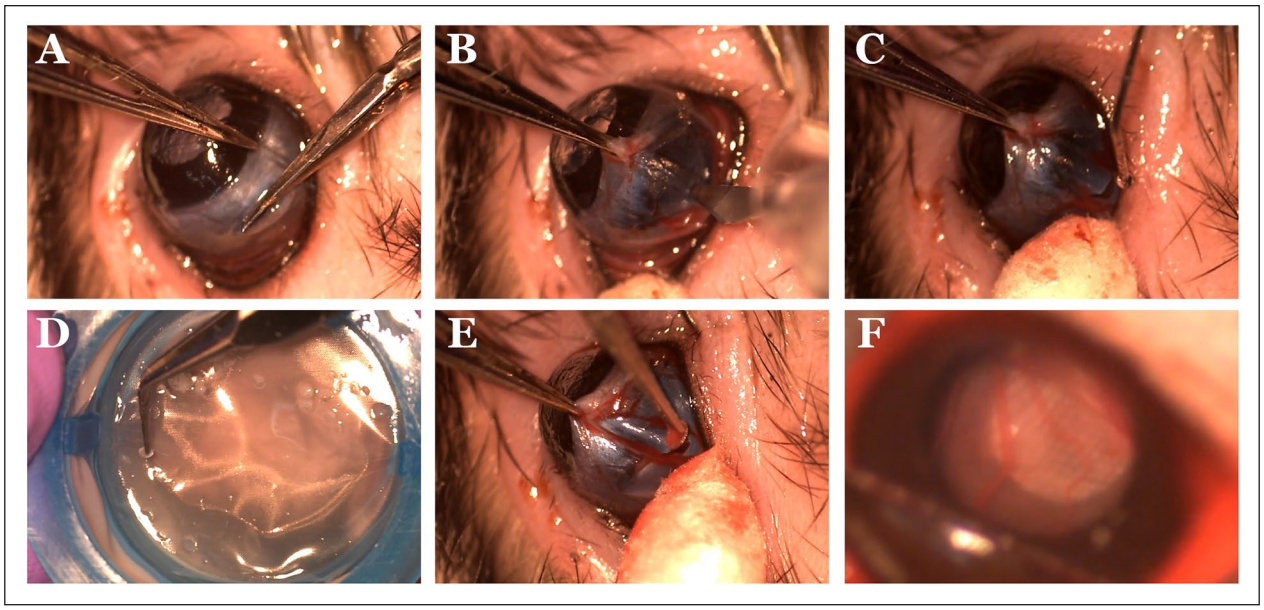

Figure 1. Surgical placement of DTVRF-hiPSC-ARG into the subretinal space of athymic nude RNU rats. (A–C) The surgical procedures required to prepare the RNU rat eye for subretinal placement of DTVRF-hiPSC-ARG. (D) The surgeon retrieving a 1-mm DTVRF-hiPSC-ARG from the transport container immediately prior to subretinal transplantation. (E) Surgical placement of a 1-mm DTVRF-hiPSC-ARG through a transscleral incision into the subretinal space of the RNU rat. (F) Image depicting DTVRF-hiPSC-ARG immediately following placement into the subretinal space of an RNU rat. RNU: Rowett Nude.

into the subretinal space (Fig. 1E). A 30-gauge anterior chamber cannula was then inserted subretinally to push the polymer away from the incision site. The conjunctiva was then reflected over the scleral wound, which was left to close by secondary intention.

Fundus Imaging and Optical Coherence Tomography (OCT)

Rats were anesthetized with ketamine/xylazine mixture [40–100 mg/kg ketamine (Clipper Distributors, Saint Joseph, MO, USA), 5–13 mg/kg xylazine (Akorn Pharmaceuticals, Lake Forest, IL, USA)], and eyes were dilated with 1 to 2 drops of Tropicamide (Alcon Laboratories, Fort Worth, TX, USA). Prior to sacrifice for biodistribution studies or histologic evaluation (see the next section), eyes were examined by a retina specialist (I.C.H.) under an operating microscope to record clinical findings, including presence of iris synechiae (suggestive of anterior chamber inflammation), cataract formation, vitreous haze or opacities (consistent with posterior chamber inflammation), retinal reattachment, chorioretinal atrophy, and subretinal fibrosis. Fundus photographs were obtained *in vivo* using the Micron III fundus camera (Phoenix Technology Group, Pleasanton, CA, USA). OCT imaging was performed using the Bioptigen Envisu R2200 (Bioptigen, Inc., Morrisville, NC, USA) with a slit-lamp-based mount. A limbal suture was placed at the corresponding clock hour of the transplantation site for reference when embedding tissues for sectioning.

Clinical Chemistry, Hematology, and Histologic Evaluation

RNU rats were sacrificed 1, 3, and 6 months following subretinal transplantation via CO_2 inhalation followed by cervical dislocation. As indicated in Table 1, 10 rats (five male and five female) were used for each of the three posttransplant survival time points evaluated in this study. To allow for possible differences between patient-derived donor cells, four different patient iPSC lines and resulting retinal progenitor cells were used in this study for a total of 120 rats receiving iPSC-derived cells on scaffolds. Scaffold-only-injected animals were used as controls ($N = 30$, five male and dive female for each of the three survival time points, that is, 1, 3, and 6 months postsurgery). To evaluate systemic effects, blood was collected at sacrifice for hematology (Table 2) and clinical chemistry analyses (Table 3). Gross pathology was performed at necropsy, and organ weights and photos were collected. Finally, the organs listed in Table 4 were collected, embedded in paraffin, sectioned, stained with hematoxylin and eosin (H&E), and evaluated by a board-certified veterinary pathologist.

Results

DTVRF-hiPSC-ARG Fabrication

PCL triol ($M_n \sim 300$ g/mol) was functionalized via mixing with potassium carbonate and acryloyl chloride at a ratio of 1:3:3 as described in section "Materials and Methods."

Table 1. DTVRF-hiPSC-ARG Study Design.

Group	Treatment	Dose per eye	Number of rats per group	Number of animals per terminal endpoint		
				1 month	3 months	6 months
1	3D Scaffold (vehicle control)	NA	15M	5M	5M	5M
			14F	5F	5F	4F
2	DTVRF-hiPSC-ARG (P1)	1 graft—scaffold containing 40,000 cells	16M	5M	5M	6M
			15F	5F	5F	5F
3	DTVRF-hiPSC-ARG (P2)	1 graft—scaffold containing 40,000 cells	15M	5M	5M	5M
			15F	5F	5F	5F
4	DTVRF-hiPSC-ARG (P3)	1 graft—scaffold containing 40,000 cells	15M	5M	5M	5M
			15F	5F	5F	5F
5	DTVRF-hiPSC-ARG (P4)	1 graft—scaffold containing 40,000 cells	15M	5M	5M	5M
			15F	5F	5F	5F

3D Scaffold (vehicle control): animals received a single 1-mm cell delivery scaffold, which are used to construct DTVRF-hiPSC-ARG, via subretinal transplantation without any human induced pluripotent stem cells-derived retinal progenitor cells loaded onto it. DTVRF-hiPSC-ARG: animals received a single 1-mm retinal cell graft via subretinal transplantation that contained induced pluripotent stem cells-derived photoreceptor precursor cells generated from four independent individuals, one with no disease and three with rod-selective photoreceptor cell disease (ie, each of these individuals have normal cone cells).

Table 2. List of Hematology Tests Performed at 1, 3, and 6 Months Following Subretinal Transplantation of Engineered Human Retinal Progenitor Cell Grafts in Immunocompromised Rowett Nude Rats.

Red blood cells (M/μl)	Neutrophils (K/μl)
Hemoglobin (g/dl)	Neutrophils (%)
Hematocrit (%)	Lymphocytes (K/μl)
Mean corpuscular volume (fl)	Lymphocytes (%)
Mean corpuscular hemoglobin (pg)	Monocytes (K/μl)
Mean corpuscular hemoglobin concentration (g/dl)	Monocytes (%)
Red cell distribution width (%)	Eosinophils (K/μl)
Reticulocytes (K/μl)	Eosinophils (%)
Reticulocytes (%)	Basophils (K/μl)
Platelet count (K/μl)	Basophils (%)
White blood cells (K/μl)	

Table 3. List of Clinical Chemistry Tests Performed at 1, 3, and 6 Months Following Subretinal Transplantation of Engineered Human Retinal Progenitor Cell Grafts in Immunocompromised Rowett Nude Rats.

Total protein (g/dl)	Lactate dehydrogenase (U/l)
Albumin (g/dl)	Total bilirubin (mg/dl)
Globulin (g/dl)	Phosphorus (mg/dl)
Sodium (mmol/l)	Blood urea nitrogen (mg/dl)
Potassium (mmol/l)	Creatinine (mg/dl)
Chloride (mmol/l)	Cholesterol (mg/dl)
Total CO_2 (mmol/l)	Triglycerides (mg/dl)
Calcium (mg/dl)	Creatine kinase (U/l)
Glucose (mg/dl)	Uric acid (mg/dl)
Alkaline phosphatase (U/l)	HDL (mg/dl)
Alanine aminotransferase (U/l)	LDL (mg/dl)
Aspartate aminotransferase (U/l)	

HDL: high-density lipoprotein; LDL: low-density lipoprotein.

Table 4. List of Tissues Weighed and Evaluated at 1, 3, and 6 Months Following Subretinal Transplantation of Engineered Human Retinal Progenitor Cell Grafts in Immunocompromised Rowett Nude Rats.

Tissue	Organ weights	Gross photo	Microscopic examination
Nose			X
Ethmoid sinus			X
Tongue			X
Salivary glands			X
Teeth			X
Skeletal muscle			X
Ear (bulla)			X
Peripheral nerve (head)			X
Harderian glands			X
Bone			X
Bone marrow			X
Pituitary gland			X
Brain (parasagittal section)	X	X	X
Eyes (with optic nerves)			X
Spleen	X	X	X
Liver	X	X	X
Abdominal skin		X	X
Mammary glands			X
Stomach		X	X
Pancreas	X	X	X
Lymph node (mesenteric)		X	X
Anterior prostate		X	X
Testis		X	X
Epididymis		X	X
Seminal vesicle		X	X
Vas deferens		X	X
Vagina		X	X
Uterus		X	X
Ovary		X	X
Oviduct		X	X
Urinary bladder		X	X
Duodenum		X	X
Jejunum		X	X
Ileum		X	X
Cecum		X	X
Proximal Colon		X	X
Distal colon		X	X
Bone (femur, tibia, fibula)		X	X
Bone marrow			X
Skeletal muscle (biceps femoris)		X	X
Sciatic nerve		X	X
Sternum		X	X
Spine—cervical		X	
Spine—thoracic		X	X
Spine—lumbar		X	
Lungs	X	X	X
Larynx		X	X
Trachea		X	X
Aorta		X	X
Esophagus		X	X
Ureter		X	X
Adrenal gland		X	X
Thyroid gland		X	X
Parathyroid gland		X	X
Heart	X	X	X
Brown adipose tissue			X
White adipose tissue			X
Kidney	X	X	X
Thymus	X	X	X

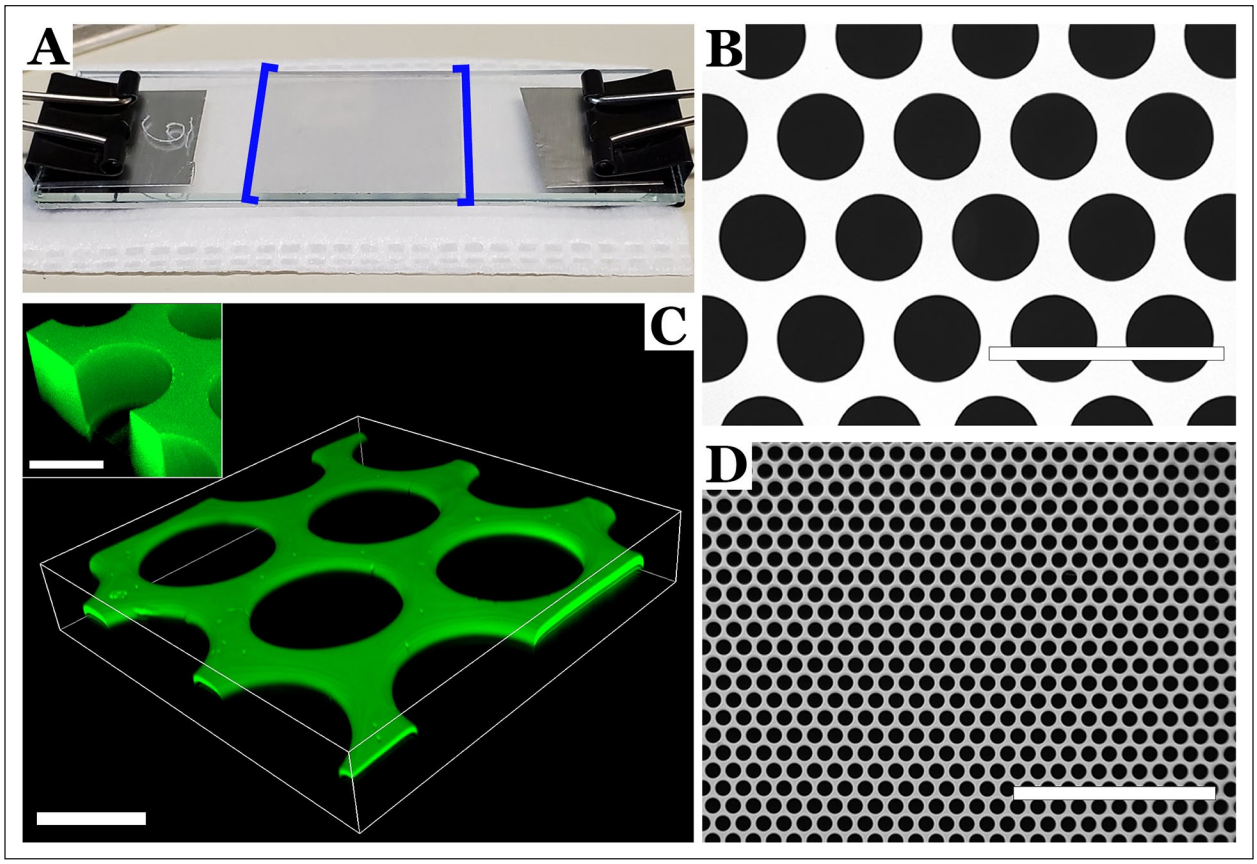

Figure 2. Fabrication of polycaprolactone cell delivery scaffolds via ultraviolet polymerization. (A) The scaffold fabrication chamber. (B) Phase micrograph of the photomask used to create pores in the polycaprolactone cell delivery scaffold. This photomask can be seen as a gray square denoted by blue brackets on the upper layer of the fabrication chamber shown in panel A. Confocal (C) and scanning electron (D) micrographs of the polycaprolactone scaffold following fabrication. Scale bar = 100 µm (B), 50 µm (C), and 1 mm (D).

To generate PCL-cell-delivery scaffolds, functionalized PCL was injected into a custom polymerization mold and exposed to UV light at an intensity approximately 100 lumens/cm^2. The polymerization chamber consists of two glass slides separated by two 50-µm spacers placed approximately 2.5 cm apart (Fig. 2A). The upper slide was covered by a photomask containing 75-µm black spots spaced at 25-µm intervals with adjacent spots aligned in a hexagonal pattern (Fig. 2B). The photomask was designed to block UV light and prevent polymerization, thereby creating pores in the resulting polymerized scaffold. Following polymerization, the chamber was disassembled, and the polymerized scaffold was washed to remove residual unpolymerized prepolymer. Scaffolds were subsequently sterilized via gamma irradiation (25,000 Gray for approximately 18 h) before being returned to a cGMP compliant BioSpherix cell culture system for seeding with patient iPSC-derived retinal progenitor cells (iPSC-RPCs). As determined via both confocal microscopy (Fig. 2C) and scanning electron microscopy (Fig. 2D), the resulting scaffolds were 50-µm thick and contained full-thickness pores that were 60 µm in diameter.

Following sterilization, PCL scaffolds were coated with Laminin 521 and seeded with patient iPSC-derived retinal progenitor cells harvested from retinal organoids differentiated for approximately 80 days as described in section "Materials and Methods." At this point in time, retinal organoids largely contain retinal progenitor cells that express markers such as SOX2 and CHX10 (Fig. 3A, B). If differentiated for an additional 70 days, these cells give rise to both NR2E3-, NRL-, and rhodopsin-positive rod photoreceptor cells and ARR3- and blue opsin-positive cone photoreceptor cells (Fig. 3C–E). As shown in Fig. 3F, 14 days following seeding (ie, ~94 days post-differentiation) scaffolds were densely packed with iPSC-RPCs. At this time point, approximately 70% of the cells expressed the photoreceptor precursor cell markers OTX2 (Fig. 3G, H) and Recoverin (Fig. 3I, J). Although some retinal progenitor cells did adhere to the surface of the polymer, most of the cells were located within the 60-µm vertical pores of the scaffold (Fig. 3J).

Subretinal Transplantation and Analysis of DTVRF-hiPSC-ARG Tolerability

To evaluate local and systemic compatibility of DTVRF-hiPSC-ARG, 1-mm grafts were transplanted into the subretinal space of immunodeficient RNU rats as described in

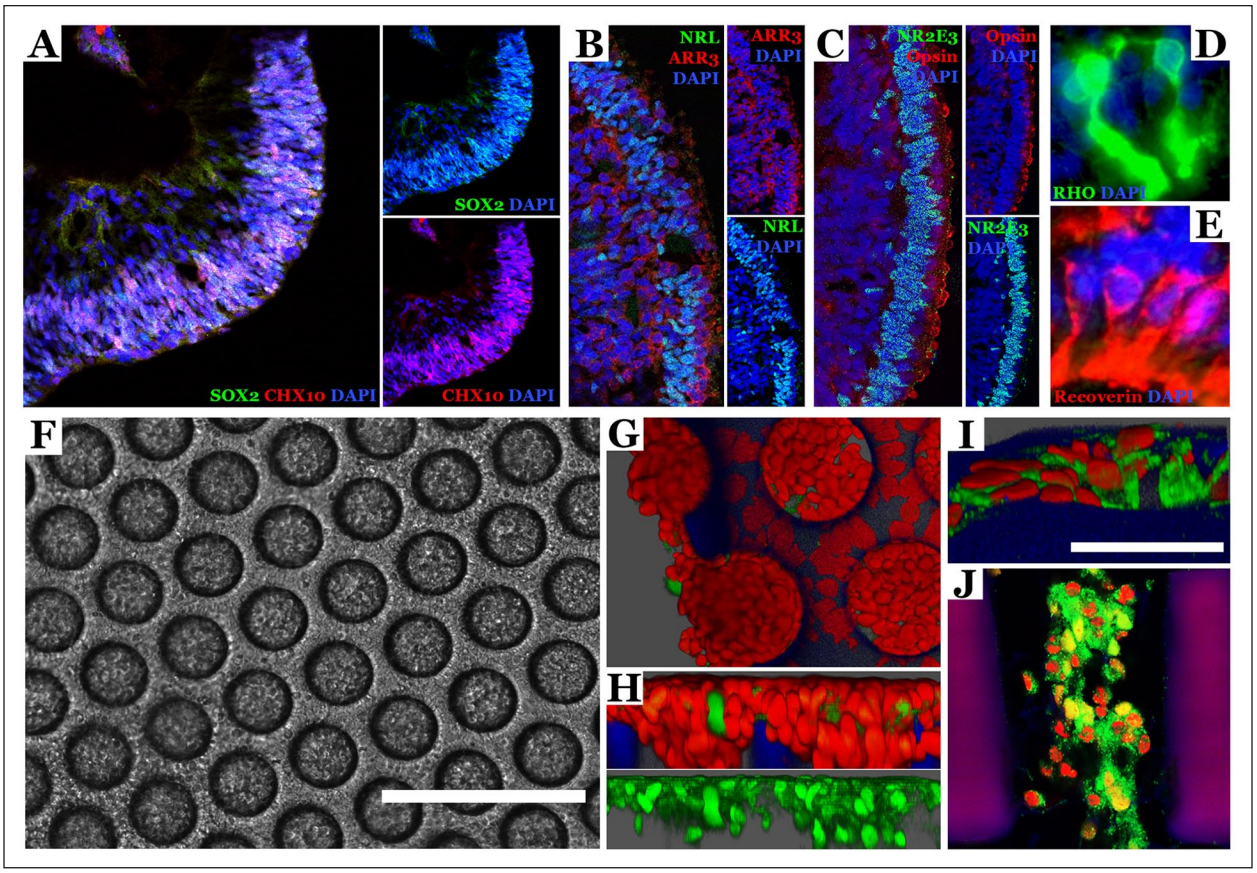

Figure 3. Generation of DTVRF-hiPSC-ARGs via seeding of PCL scaffolds with patient iPSC-derived retinal progenitor cells. (A–E) Immunocytochemical staining of hiPSC-derived retinal organoids at differentiation days 80 (A—time of dissociation and scaffold seeding) and 150 (B–E). Antibodies targeting the retinal progenitor cell markers SOX2 and CHX10, the rod photoreceptor cell markers NR2E3, NRL, and rhodopsin, and the cone photoreceptor cell markers ARR3 and blue cone opsin. DAPI was used as a nuclear counterstain. (F) Phase micrograph of DTVRF-hiPSC-ARG 2 weeks following seeding. Note the uniform seeding of pores across the entire scaffold. (G–J) Immunocytochemical staining of DTVRF-hiPSC-ARG 2 weeks following seeding. Antibodies targeting OTX2 (G and H—green) and Recoverin (I and J—green) were used to confirm the presence of photoreceptor precursor cells. Red = Sytox™ nuclear stain. Scale bar = 200 µm (F) and 50 µm (I). The scaffold material autofluoresces blue-magenta under these conditions. PCL: polycaprolactone; iPSC: induced pluripotent stem cells; hiPSC: human induced pluripotent stem cell.

section "Materials and Methods." As shown in Table 1, 10 rats (five male and five female) were sacrificed at each of three posttransplant survival times (1, 3, and 6 months, N = 30 per patient for a total of 120 rats). Scaffold only transplanted animals were used as vehicle controls (N = 30, that is, five male and five female, each sacrificed at 1, 3, and 6 months postsurgery). Prior to sacrifice, a clinical ophthalmic exam was performed, and clinical findings were recorded. Unfortunately, RNU rats are prone to developing prolapsed eyelashes and corneal clouding with age, and as a result a clear view of the fundus was not possible for the majority of the animals 3 and 6 months following transplant. However, in cases where the cornea was clear, no evidence of iris synechiae (suggestive of anterior chamber inflammation), vitreous haze or opacities (consistent with posterior chamber inflammation), retinal detachment, or chorioretinal atrophy was identified. As shown by both fundus photography (Fig. 4A) and OCT (Fig. 4B), 1 month following transplant, the host retina had reattached, and no evidence of abnormal donor cell proliferation, tumor formation, or toxicity to adjacent retinal tissue was detected. To augment these clinical data an additional small cohort of rats (n = 3) was sacrificed 6 months following transplant and the eyes were harvested and subjected to histological examination in addition to the animals subjected to detailed histopathologic study as part of the original study design.

As shown in Fig. 4C, while the outer nuclear layer (ONL) immediately above the implant (marked by blue dashed square) was disrupted as one would expect with transplantation into a non-diseased model, the host retina adjacent to the implant was normal. Specifically, the outer nuclear layer, photoreceptor cell inner and outer segments (Fig. 4C black *, D), RPE cell layer (Fig. 4C, arrowheads) and choroid remained intact. In fact, the host RPE cell layer and

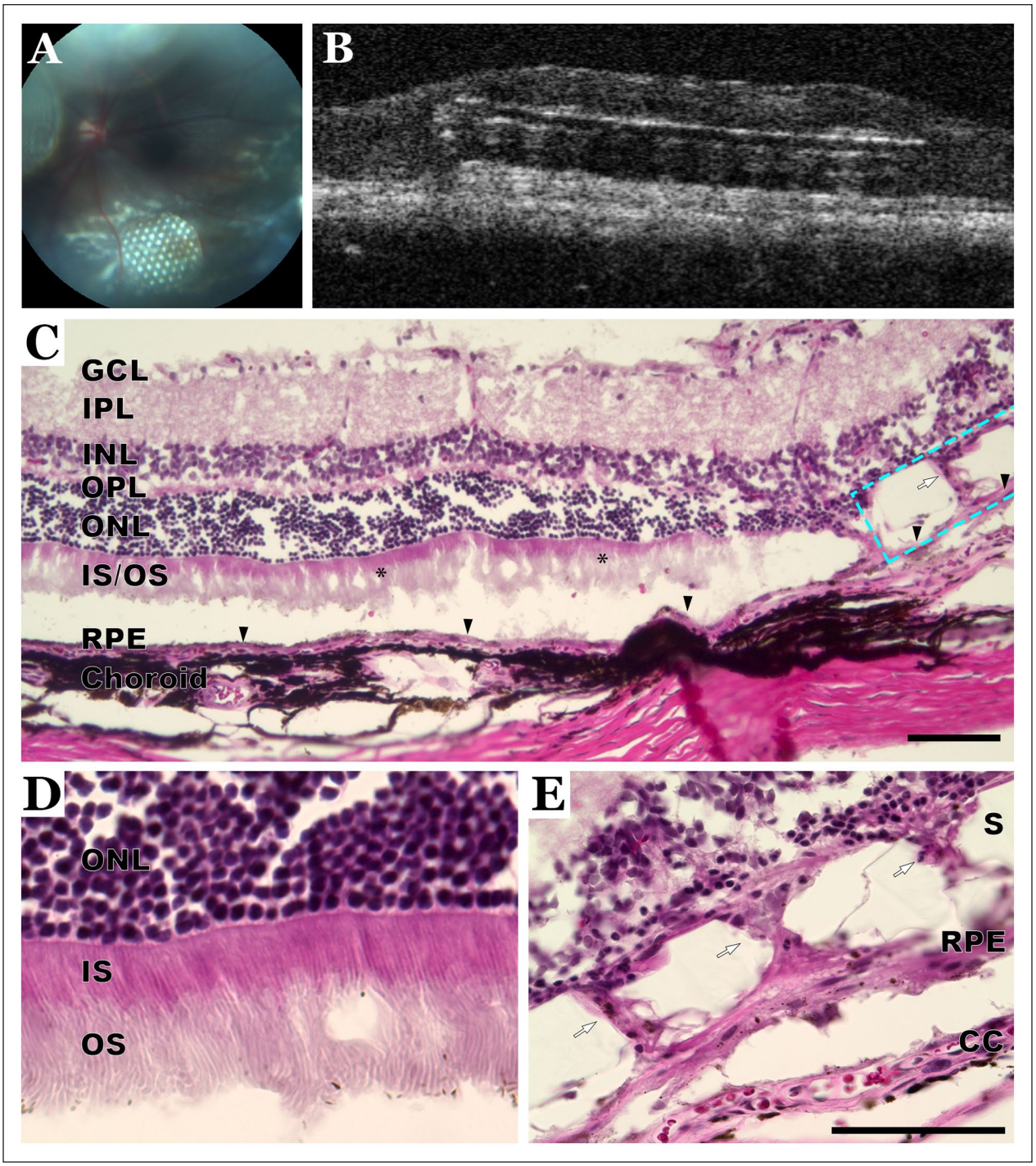

Figure 4. Local tolerability of DTVRF-hiPSC-ARG. Fundus photo (A) and optical coherence tomogram (B) 1 month following subretinal placement of DTVRF-hiPSC-ARG in an RNU rat. (C–E) H&E staining of RNU rat eye at 6 months following subretinal placement. Note the intact photoreceptor cell outer nuclear layer, inner segments, and outer segments adjacent to the polymer (D). Scale bar = 100 µm. White arrows denote full-thickness pores in the PCL scaffold. Black arrowheads denote the RPE cell layer. Black * denotes photoreceptor inner and outer segments. Blue dashed box denotes polymer scaffold. RNU: Rowett Nude; PCL: polycaprolactone; RPE: retinal pigmented epithelial; CC: choriocapillaris; GCL: ganglion cell layer; IPL: inner plexiform layer; INL: inner nuclear layer; OPL: outer plexiform layer; ONL: outer nuclear layer; IS/OS: photoreceptor cell inner and outer segment layer; IS: inner segments; OS: outer segments; S: scaffold.

choroid were preserved immediately beneath the implant (Fig. 4C, E). Finally, cells were detected both on top of the scaffold and within the vertical pores, which as depicted in Fig. 2 is precisely where they were seeded (Fig. 4E, arrows). Collectively, these data demonstrate that 3D human iPSC-derived retinal progenitor cell grafts (ie, DTVRF-hiPSC-ARG) are well tolerated locally.

To evaluate systemic tolerability, blood was collected at the time of sacrifice for hematology and clinical chemistry. Organs were removed, carefully examined, weighed, fixed, and paraffin embedded. All tissues, including the head with eyes, were subsequently sectioned, H&E stained and subjected to detailed histopathology by a veterinarian pathologist. While sporadic differences were detected in several of the hematology (Table 5, significant differences highlighted) and clinical chemistry (Table 6) parameters, no evidence of DTVRF-hiPSC-ARG induced toxicity was detected at 1-, 3-, or 6-month post-subretinal transplant. Likewise, no evidence of tumor formation or DTVRF-hiPSC-ARG induced toxicity was detected in any animal via gross pathology (Table 7). Similarly, as shown in Table 8, while the thymus of 1-month female and the pancreas of 3-month female animals that received P3 were significantly heavier than those of vehicle control animals at the same posttransplant time point, no donor cell proliferation, tumor formation, or other histopathologic abnormalities were seen in these organs. In fact, no evidence of tumorigenicity, tissue necrosis, or toxicity was detected in any of the animals studied with detailed histopathology (Table 9). Collectively, these data demonstrate that DTVRF-hiPSC-ARG is well tolerated systemically for up to 6 months following transplant.

Discussion

There is growing evidence that pluripotent stem cell-derived retinal progenitor cells can restore retinal function following subretinal transplantation[2–15], and as a result, the field is rapidly progressing toward human clinical trials. However, before initiating such human trials, it is essential to demonstrate that the proposed treatment has a favorable safety profile in preclinical studies. A concern often associated with the use of pluripotent stem cells for clinical human cell replacement therapy is the potential for residual undifferentiated stem cells within the transplant to form tumors known as teratomas that contain cells of all three embryonic germ layers. Although teratomas are benign and the likelihood of undifferentiated cells leaving the eye and giving rise to tumors in extraocular tissues is very low, the possibility of forming a mass within the eye is a real concern[2]. Fortunately, retinal differentiation protocols have evolved to the point where contaminating pluripotent stem cells is rare[48,52–59]. In addition, stringent release testing strategies designed to detect cells with tumorigenic potential prior to transplantation have been developed[48,60]. Also, one of the advantages of performing the first in human clinical trials in the eye is that the transplant can be safely and inexpensively observed with biomicroscopy and optical coherence tomography at frequent intervals following transplantation. In the unlikely event that a tumor did form within the eye, it could be easily destroyed with laser photocoagulation as is done routinely for the small retinal hemangioblastomas associated with von Hippel Lindau disease[61,62]. Additional safety concerns with polymer-supported retinal cell grafts are the interaction between the host tissue, the scaffold, and the polymeric degradation products. Specifically, it is important to demonstrate that the transplanted polymer does not induce local tissue damage and that as it degrades, its degradation products do not injure the adjacent retina or other organs as the degradation products find their way into the systemic circulation. This is especially important given that polymers that undergo rapid bulk degradation, such as poly lactic-*co*-glycolic acid (PLGA), have been shown to significantly lower local pH and cause widespread retinal injury when delivered in sufficient quantities[63].

When selecting an animal model for evaluating the safety of a new 3D polymer-supported retinal cell graft, several considerations were made. First, the animal needed to have an eye that is large enough to receive a human equivalent dose of patient iPSC-derived retinal progenitor cells. Second, the animal needed to be immunocompromised to prevent acute xenograft rejection following transplantation. In previous polymer-scaffold-only studies, we utilized the Pro23His rhodopsin transgenic pig model of retinal degeneration to evaluate local and systemic tolerability[37]. Pig eyes are similar in size to humans and are thus ideal for translational research, especially for refining surgical techniques and instrument design[37]. Unfortunately, pigs are expensive to house in large numbers and difficult to immunosuppress for extended periods of time, which makes them less than ideal for evaluating the systemic tolerability of a human cell product. Although many mouse models of inherited retinal degeneration exist, including those that have been crossed onto immunocompromised backgrounds[64], the mouse eye is too small to reliably place polymer-supported photoreceptor cell grafts into the subretinal space[64]. Unlike pigs, rats are inexpensive to house in sufficient numbers to allow for testing of multiple experimental parameters at once; and unlike mice, rats have eyes that are large enough to enable subretinal transplantation of a biodegradable retinal cell graft. Rat models of retinal degeneration have been used as recipients of full-thickness retinal sheets, polymer support RPE cell grafts, and light-sensing photovoltaic arrays[6,50,51,65]. In addition to being of sufficient size to receive a 3D subretinal graft, the rat also has a sufficient volume of blood to allow for a comprehensive hematology and clinical chemistry analysis in each animal following transplantation. For these reasons, the athymic nude RNU rat, which lacks functional T cells, was chosen for the studies described above.

Although the RNU rat can receive human cells without xenograft rejection, this animal is prone to developing

Table 5. CBC Analysis at 1, 3, and 6 Months Following Subretinal Transplantation of Engineered Human Retinal Progenitor Cell Grafts in Immunocompromised Rowett Nude Rats.

	Average	SD	Average	SD	*P*-value	Average	SD	*P*-value	Average	SD	*P*-value	Average	SD	*P*-value
Sex	M	M	M	M	M	M	M	M	M	M	M	M	M	M
Time point	1M	1M	1M	1M	1M	1M	1M	1M	1M	1M	1M	1M	1M	1M
Treatment group	Control	Control	P1	P P1	Control vs P1	P2	P2	Control vs P2	P3	P3	Control vs P3	P4	P4	Control vs P4
1M Male CBC														
RBC (M/μl)	9.11	0.41	11.44	1.04	<0.0001****	9.29	0.29	>0.9999	9.73	0.33	0.8551	8.96	0.88	>0.9999
HGB (g/dl)	16.32	0.63	19.78	2.07	0.0002***	16.52	0.56	>0.9999	16.92	0.68	0.9950	15.94	1.15	0.9999
HCT (%)	53.12	2.32	64.62	6.74	0.0004***	54.80	1.53	0.9990	56.40	2.55	0.9064	53.26	4.24	>0.9999
MCV (fl)	58.32	0.76	56.42	1.28	0.1278	58.98	0.54	0.1278	57.96	1.28	0.1278	59.64	3.17	0.1278
MCH (pg)	17.90	0.21	17.26	0.29	0.1608	17.76	0.21	0.9998	17.40	0.23	0.4660	17.82	0.68	>0.9999
MCHC (g/dl)	30.72	0.48	30.60	0.37	>0.9999	30.16	0.50	0.9590	30.04	0.69	0.8772	29.96	0.56	0.7912
RDW-CV (%)	21.56	0.77	25.36	1.15	<0.0001****	21.24	0.61	>0.9999	21.78	0.77	>0.9999	20.68	1.15	0.9482
RET (K/μl)	278.92	48.41	322.28	31.45	0.1140	275.50	48.48	0.1140	304.20	13.52	0.1140	277.34	44.19	0.1140
RET (%)	3.07	0.57	2.82	0.18	0.4044	2.96	0.49	0.4044	3.13	0.20	0.4044	3.12	0.54	0.4044
PLT (K/μl)	437.80	134.17	272.40	82.64	>0.9999	529.60	47.73	>0.9999	532.60	74.65	>0.9999	409.60	58.32	>0.9999
WBC (K/μl)	4.61	0.66	8.72	0.98	0.0114*	4.86	1.44	>0.9999	3.93	1.08	0.9996	4.16	2.50	>0.9999
NEUT (K/μl)	1.20	0.34	2.79	0.79	0.0399*	1.30	0.70	>0.9999	0.95	0.37	>0.9999	1.24	0.86	>0.9999
NEUT (%)	25.78	4.47	32.32	9.08	0.2189	26.04	8.66	0.2189	24.12	5.08	0.2189	32.06	14.42	0.2189
LYMPH (K/μl)	2.79	0.34	5.16	1.04	0.0235*	2.95	0.90	>0.9999	2.60	0.63	>0.9999	2.59	1.59	>0.9999
LYMPH (%)	60.78	5.55	59.04	7.80	0.4903	61.14	6.75	0.4903	66.76	3.40	0.4903	60.44	11.08	0.4903
MONO (K/μl)	0.34	0.11	0.65	0.17	0.0999	0.39	0.15	>0.9999	0.19	0.08	0.9167	0.22	0.15	0.9744
MONO (%)	7.28	2.21	7.42	1.31	0.3438	7.96	1.78	0.3438	4.86	1.74	0.3438	4.86	1.95	0.3438
EO (K/μl)	0.23	0.15	0.11	0.10	0.0773	0.17	0.11	0.0773	0.09	0.02	0.0773	0.09	0.12	0.0773
EO (%)	4.80	2.90	1.22	1.02	0.1231	4.06	3.24	0.1231	2.32	0.58	0.1231	1.94	2.38	0.1231
BASO (K/μl)	0.06	0.04	0.00	0.00	0.2145	0.04	0.06	0.2145	0.09	0.09	0.2145	0.03	0.05	0.2145
BASO (%)	1.36	0.88	0.00	0.00	0.4286	0.80	0.86	0.4286	1.94	1.79	0.4286	0.70	1.10	0.4286
	Average	SD	Average	SD	*P*-value	Average	SD	*P*-value	Average	SD	*P*-value	Average	SD	*P*-value
Sex	F	F	F	F	F	F	F	F	F	F	F	F	F	F
Time point	1 M	1 M	1 M	1 M	1 M	1 M	1 M	1 M	1 M	1 M	1 M	1 M	1 M	1 M
Treatment group	Control	Control	P1	P P1	Control vs P1	P2	P2	Control vs P2	P3	P3	Control vs P3	P4	P4	Control vs P4
1M Female CBC														
RBC (M/μl)	8.88	0.57	10.71	0.19	0.0014**	8.70	0.65	>0.9999	9.03	0.67	>0.9999	8.90	0.67	>0.9999
HGB (g/dl)	15.82	0.94	18.38	0.19	0.0115*	15.14	0.79	0.9878	15.82	0.96	>0.9999	15.84	1.21	>0.9999
HCT (%)	52.76	3.35	63.06	1.01	0.0019**	51.38	3.52	0.9998	52.38	3.87	>0.9999	51.44	3.49	0.9999
MCV (fl)	59.36	0.51	58.88	0.86	0.1278	59.10	0.80	0.1278	58.06	2.98	0.1278	57.86	1.38	0.1278
MCH (pg)	17.80	0.28	17.20	0.12	0.2273	17.44	0.57	0.8440	17.52	0.30	0.9612	17.80	0.27	>0.9999
MCHC (g/dl)	29.98	0.30	29.14	0.35	0.6853	29.48	0.74	0.9801	30.26	1.26	0.9997	30.80	1.13	0.7131
RDW-CV (%)	18.78	1.13	21.84	0.48	0.0020**	18.10	1.66	0.9904	19.98	1.23	0.7485	20.08	1.23	0.6570
RET (K/μl)	239.32	34.13	266.06	49.09	0.1140	251.92	30.17	0.1140	240.30	48.28	0.1140	273.02	71.77	0.1140
RET (%)	2.69	0.25	2.48	0.43	0.4044	2.92	0.50	0.4044	2.66	0.45	0.4044	3.09	0.85	0.4044
PLT (K/μl)	608.40	166.83	559.80	343.53	>0.9999	517.80	126.82	>0.9999	472.40	50.01	>0.9999	411.80	50.16	>0.9999
WBC (K/μl)	3.69	1.60	4.80	2.50	0.9863	3.08	1.68	0.9999	2.63	1.16	0.9901	3.45	1.91	>0.9999
NEUT (K/μl)	1.02	0.63	1.91	1.40	0.6520	0.87	0.69	>0.9999	0.45	0.34	0.9657	0.97	0.55	>0.9999
NEUT (%)	23.74	13.00	34.94	18.08	0.2189	25.86	10.50	0.2189	15.46	6.44	0.2189	29.04	6.04	0.2189
LYMPH (K/μl)	2.23	0.99	2.47	1.27	>0.9999	1.90	0.93	>0.9999	1.81	0.80	0.9997	2.14	1.26	>0.9999
LYMPH (%)	59.92	3.82	56.46	15.49	0.4903	63.84	7.47	0.4903	68.28	5.85	0.4903	60.38	7.54	0.4903
MONO (K/μl)	0.28	0.16	0.30	0.26	>0.9999	0.24	0.16	>0.9999	0.22	0.14	0.9998	0.28	0.19	>0.9999
MONO (%)	7.54	1.80	6.12	3.67	0.3438	7.74	2.89	0.3438	8.22	3.62	0.3438	7.40	3.16	0.3438
EO (K/μl)	0.09	0.07	0.07	0.05	0.0773	0.06	0.01	0.0773	0.14	0.08	0.0773	0.06	0.06	0.0773
EO (%)	2.98	2.09	1.70	0.89	0.1231	2.30	1.27	0.1231	7.96	8.24	0.1231	2.92	3.95	0.1231
BASO (K/μl)	0.07	0.11	0.05	0.10	0.2145	0.00	0.01	0.2145	0.00	0.00	0.2145	0.00	0.01	0.2145
BASO (%)	5.82	11.67	0.78	1.39	0.4286	0.26	0.40	0.4286	0.08	0.18	0.4286	0.26	0.58	0.4286

(continued)

Table 5. (continued)

	Average	SD	Average	SD	*P*-value	Average	SD	*P*-value	Average	SD	*P*-value	Average	SD	*P*-value
Sex	M	M	M	M	M	M	M	M	M	M	M	M	M	M
Time point	3 M	3 M	3 M	3 M	3 M	3 M	3 M	3 M	3 M	3 M	3 M	3 M	3 M	3 M
Treatment group	Control	Control	P1	P P1	Control vs P1	P2	P2	Control vs P2	P3	P3	Control vs P3	P4	P4	Control vs P4
3M Male CBC														
RBC (M/μl)	10.07	0.84	9.07	0.50	0.2018	9.81	0.71	0.9994	9.68	0.84	0.9864	9.39	0.78	0.7090
HGB (g/dl)	17.02	1.45	15.80	0.51	0.0580	17.00	1.25	0.0580	16.68	0.75	0.0580	16.52	1.23	0.0580
HCT (%)	55.70	5.16	50.64	3.58	0.2769	56.08	4.75	0.2769	55.08	3.57	0.2769	54.58	5.30	0.2769
MCV (fl)	55.30	1.96	55.78	1.30	>0.9999	57.16	2.33	0.9124	57.08	4.18	0.9315	58.04	1.59	0.5401
MCH (pg)	16.90	0.63	17.42	0.50	0.0524	17.32	0.28	0.0524	17.28	0.99	0.0524	17.60	0.43	0.0524
MCHC (g/dl)	30.58	0.47	31.26	1.24	0.1765	30.36	0.78	0.1765	30.34	1.05	0.1765	30.32	0.79	0.1765
RDW-CV (%)	23.38	1.34	22.00	0.83	0.5104	22.68	1.27	0.9833	22.86	1.59	0.9981	21.62	0.86	0.1956
RET (K/μl)	247.52	19.95	224.54	38.30	0.5556	231.48	37.51	0.5556	229.50	32.76	0.5556	255.22	60.66	0.5556
RET (%)	2.47	0.24	2.48	0.42	0.3533	2.35	0.22	0.3533	2.40	0.50	0.3533	2.69	0.41	0.3533
PLT (K/μl)	708.00	72.47	414.20	104.54	0.0040**	389.60	117.74	0.0014**	497.20	131.62	0.0954	347.60	49.27	0.0002***
WBC (K/μl)	5.82	0.99	3.93	1.54	0.5617	4.22	1.47	0.5617	4.75	0.76	0.5617	5.36	2.31	0.5617
NEUT (K/μl)	1.56	0.82	0.75	0.33	0.5390	1.04	0.30	0.5390	1.10	0.13	0.5390	1.50	0.85	0.5390
NEUT (%)	26.80	12.42	18.72	2.46	0.7630	25.34	3.26	0.7630	23.58	3.38	0.7630	27.40	6.38	0.7630
LYMPH (K/μl)	3.21	0.91	2.44	1.03	0.9401	2.71	1.01	0.9401	2.99	0.66	0.9401	3.33	1.44	0.9401
LYMPH (%)	55.20	12.05	61.18	6.70	0.6275	63.74	3.23	0.6275	62.44	5.26	0.6275	61.46	5.74	0.6275
MONO (K/μl)	0.52	0.16	0.30	0.18	0.3706	0.36	0.18	0.3706	0.35	0.09	0.3706	0.40	0.19	0.3706
MONO (%)	8.82	1.90	7.00	2.19	0.7454	8.22	2.21	0.7454	7.32	1.01	0.7454	7.88	2.17	0.7454
EO (K/μl)	0.45	0.38	0.38	0.24	0.9994	0.09	0.06	0.0377	0.23	0.20	0.5382	0.11	0.06	0.0609
EO (%)	7.68	6.34	11.24	10.06	0.9531	2.18	1.20	0.6216	5.02	4.11	0.9933	2.62	1.62	0.7220
BASO (K/μl)	0.09	0.05	0.07	0.07	>0.9999	0.02	0.03	0.3377	0.07	0.09	0.9995	0.02	0.03	0.3377
BASO (%)	1.50	0.64	1.86	1.24	0.1182	0.52	0.94	0.1182	1.64	2.07	0.1182	0.64	0.97	0.1182
	Average	SD	Average	SD	*P*-value	Average	SD	*P*-value	Average	SD	*P*-value	Average	SD	*P*-value
Sex	F	F	F	F	F	F	F	F	F	F	F	F	F	F
Time point	3 M	3 M	3 M	3 M	3 M	3 M	3 M	3 M	3 M	3 M	3 M	3 M	3 M	3 M
Treatment group	Control	Control	P1	P P1	Control vs P1	P2	P2	Control vs P2	P3	P3	Control vs P3	P4	P4	Control vs P4
3M Female CBC														
RBC (M/μl)	8.99	0.21	8.76	0.39	0.9998	9.15	0.21	>0.9999	9.05	0.39	>0.9999	8.95	0.41	>0.9999
HGB (g/dl)	16.14	0.28	15.40	0.73	0.0580	15.72	0.45	0.0580	16.06	0.71	0.0580	15.84	0.54	0.0580
HCT (%)	53.76	1.43	50.60	3.52	0.2769	53.26	2.00	0.2769	53.66	3.58	0.2769	52.70	2.54	0.2769
MCV (fl)	59.78	0.95	57.70	2.26	0.8441	58.20	0.83	0.9665	59.22	1.88	>0.9999	58.88	1.18	0.9994
MCH (pg)	17.94	0.21	17.56	0.32	0.0524	17.20	0.24	0.0524	17.76	0.17	0.0524	17.70	0.29	0.0524
MCHC (g/dl)	30.02	0.48	30.48	0.84	0.1765	29.54	0.62	0.1765	29.96	0.86	0.1765	30.06	0.82	0.1765
RDW-CV (%)	19.24	0.96	19.54	0.62	>0.9999	19.66	0.48	0.9996	19.88	0.45	0.9910	18.82	1.12	0.9996
RET (K/μl)	236.92	56.95	256.64	58.10	0.5556	211.56	25.21	0.5556	238.44	30.61	0.5556	200.68	46.93	0.5556
RET (%)	2.63	0.57	2.92	0.61	0.3533	2.31	0.24	0.3533	2.64	0.36	0.3533	2.24	0.50	0.3533
PLT (K/μl)	511.60	80.83	470.80	110.30	0.9998	485.20	72.79	>0.9999	558.00	88.09	0.9995	470.60	189.82	0.9998
WBC (K/μl)	3.98	1.47	4.49	1.34	0.5617	3.83	2.02	0.5617	4.34	0.86	0.5617	4.12	2.09	0.5617
NEUT (K/μl)	0.93	0.86	1.30	0.72	0.5390	0.96	0.51	0.5390	1.06	0.46	0.5390	1.03	0.55	0.5390
NEUT (%)	22.46	12.85	28.60	10.27	0.7630	25.66	5.74	0.7630	24.54	9.06	0.7630	24.86	2.96	0.7630
LYMPH (K/μl)	2.57	1.01	2.82	0.85	0.9401	2.50	1.35	0.9401	2.81	0.74	0.9401	2.73	1.39	0.9401
LYMPH (%)	64.68	10.89	62.60	10.55	0.6275	64.78	4.04	0.6275	64.16	8.60	0.6275	66.26	3.43	0.6275
MONO (K/μl)	0.30	0.14	0.28	0.05	0.3706	0.30	0.17	0.3706	0.31	0.11	0.3706	0.31	0.17	0.3706
MONO (%)	7.64	2.05	6.52	1.08	0.7454	7.66	1.26	0.7454	7.16	2.07	0.7454	7.40	1.39	0.7454
EO (K/μl)	0.15	0.08	0.08	0.03	0.9992	0.05	0.03	0.9933	0.14	0.11	>0.9999	0.05	0.02	0.9898
EO (%)	4.62	3.94	2.04	1.34	0.9946	1.42	0.33	0.9760	3.62	3.77	>0.9999	1.32	0.54	0.9707
BASO (K/μl)	0.03	0.04	0.01	0.03	>0.9999	0.02	0.03	>0.9999	0.02	0.04	>0.9999	0.00	0.01	0.9990
BASO (%)	0.60	0.87	0.24	0.54	0.1182	0.48	0.78	0.1182	0.52	1.05	0.1182	0.16	0.26	0.1182

(continued)

Table 5. (continued)

	Average	SD	Average	SD	*P*-value	Average	SD	*P*-value	Average	SD	*P*-value	Average	SD	*P*-value
Sex	M	M	M	M	M	M	M	M	M	M	M	M	M	M
Time point	6 M	6 M	6 M	6 M	6 M	6 M	6 M	6 M	6 M	6 M	6 M	6 M	6 M	6 M
Treatment group	Control	Control	P1	P P1	Control vs P1	P2	P2	Control vs P2	P3	P3	Control vs P3	P4	P4	Control vs P4
6M Male CBC														
RBC (M/μl)	9.32	0.62	9.19	0.40	>0.9999	10.24	0.35	0.3081	9.37	0.52	>0.9999	10.09	0.98	0.5686
HGB (g/dl)	15.98	0.85	15.87	0.61	>0.9999	17.42	0.90	0.3813	15.84	0.58	>0.9999	17.34	1.56	0.4679
HCT (%)	52.22	4.61	52.33	1.92	>0.9999	56.80	2.97	0.7011	51.12	2.70	>0.9999	58.20	5.93	0.3119
MCV (fl)	55.98	1.72	57.00	1.87	0.9950	55.42	1.46	>0.9999	54.56	0.76	0.9546	57.66	0.51	0.8706
MCH (pg)	17.16	0.41	17.28	0.55	>0.9999	17.00	0.37	>0.9999	16.92	0.63	0.9993	17.18	0.24	>0.9999
MCHC (g/dl)	30.68	1.02	30.33	0.69	0.0680	30.66	0.42	0.0680	30.98	0.91	0.0680	29.82	0.64	0.0680
RDW-CV (%)	22.48	0.86	21.87	0.78	0.9961	23.70	0.36	0.7146	22.84	1.05	>0.9999	23.00	1.35	0.9994
RET (K/μl)	216.28	28.94	234.53	29.33	0.9053	242.90	36.36	0.9053	258.48	52.26	0.9053	261.42	43.20	0.9053
RET (%)	2.31	0.17	2.55	0.26	0.8516	2.37	0.32	0.8516	2.78	0.71	0.8516	2.58	0.28	0.8516
PLT (K/μl)	288.60	201.39	386.00	84.02	0.9977	218.20	193.64	>0.9999	301.80	177.27	>0.9999	257.60	94.58	>0.9999
WBC (K/μl)	4.45	2.19	6.66	3.76	0.6831	5.45	0.85	0.6831	5.56	1.26	0.6831	6.56	2.67	0.6831
NEUT (K/μl)	1.03	0.64	1.33	0.39	0.3299	1.43	0.77	0.3299	1.69	0.62	0.3299	2.01	0.64	0.3299
NEUT (%)	21.38	7.30	23.68	10.63	0.3179	25.26	10.12	0.3179	30.50	8.55	0.3179	32.52	8.33	0.3179
LYMPH (K/μl)	2.91	1.28	4.24	2.65	0.7303	3.47	0.29	0.7303	3.30	0.99	0.7303	3.90	1.84	0.7303
LYMPH (%)	67.70	7.35	62.08	5.65	0.5181	64.64	8.83	0.5181	59.54	10.09	0.5181	57.70	6.17	0.5181
MONO (K/μl)	0.35	0.27	0.62	0.59	0.7454	0.48	0.14	0.7454	0.46	0.16	0.7454	0.55	0.29	0.7454
MONO (%)	7.64	3.30	7.87	3.17	0.1955	8.88	2.50	0.1955	8.24	2.18	0.1955	8.02	3.31	0.1955
EO (K/μl)	0.08	0.06	0.11	0.10	0.9042	0.06	0.03	0.9042	0.05	0.03	0.9042	0.09	0.03	0.9042
EO (%)	1.94	1.09	1.98	2.31	0.8608	1.10	0.61	0.8608	0.90	0.58	0.8608	1.52	0.52	0.8608
BASO (K/μl)	0.07	0.09	0.36	0.35	>0.9999	0.01	0.01	>0.9999	0.05	0.05	>0.9999	0.01	0.02	>0.9999
BASO (%)	1.34	1.19	4.38	3.08	>0.9999	0.12	0.27	>0.9999	0.82	0.86	>0.9999	0.24	0.39	>0.9999
	Average	SD	Average	SD	*P*-value	Average	SD	*P*-value	Average	SD	*P*-value	Average	SD	*P*-value
Sex	F	F	F	F	F	F	F	F	F	F	F	F	F	F
Time point	6 M	6 M	6 M	6 M	6 M	6 M	6 M	6 M	6 M	6 M	6 M	6 M	6 M	6 M
Treatment group	Control	Control	P1	P P1	Control vs P1	P2	P2	Control vs P2	P3	P3	Control vs P3	P4	P4	Control vs P4
6M Female CBC														
RBC (M/μl)	9.27	0.98	8.72	0.39	0.9426	8.97	0.35	0.9996	9.04	0.28	>0.9999	9.21	0.54	>0.9999
HGB (g/dl)	16.20	1.48	15.32	0.68	0.9527	16.06	0.64	>0.9999	15.58	0.85	0.9969	16.24	0.79	>0.9999
HCT (%)	54.00	5.02	50.60	3.38	0.9600	51.88	2.17	0.9992	50.92	2.66	0.9804	54.46	3.76	>0.9999
MCV (fl)	58.33	1.78	58.00	1.53	>0.9999	57.80	0.60	>0.9999	56.30	1.87	0.7513	59.12	1.60	0.9998
MCH (pg)	17.50	0.42	17.56	0.39	>0.9999	17.88	0.26	0.9799	17.20	0.46	0.9971	17.64	0.34	>0.9999
MCHC (g/dl)	29.98	0.56	30.32	1.05	0.0680	30.96	0.30	0.0680	30.62	0.78	0.0680	29.84	0.65	0.0680
RDW-CV (%)	19.55	2.15	19.46	0.61	>0.9999	20.42	0.44	0.9723	20.78	0.33	0.7733	20.24	0.60	0.9956
RET (K/μl)	245.00	63.90	220.20	30.49	0.9053	254.48	45.91	0.9053	263.58	35.53	0.9053	277.24	39.82	0.9053
RET (%)	2.61	0.46	2.53	0.35	0.8516	2.85	0.57	0.8516	2.92	0.45	0.8516	3.03	0.52	0.8516
PLT (K/μl)	342.25	147.29	436.80	147.79	0.9993	292.40	145.14	>0.9999	323.00	170.61	>0.9999	280.40	120.25	>0.9999
WBC (K/μl)	5.32	0.51	4.42	1.38	0.6831	5.66	1.42	0.6831	5.97	2.43	0.6831	4.50	2.10	0.6831
NEUT (K/μl)	1.22	0.41	0.95	0.29	0.3299	1.66	0.99	0.3299	2.05	1.32	0.3299	1.53	1.08	0.3299
NEUT (%)	22.58	6.38	23.82	10.93	0.3179	27.34	9.65	0.3179	32.30	10.67	0.3179	32.58	7.90	0.3179
LYMPH (K/μl)	3.48	0.24	2.87	1.15	0.7303	3.18	0.38	0.7303	3.43	1.02	0.7303	2.59	0.98	0.7303
LYMPH (%)	65.80	5.80	63.48	7.85	0.5181	57.62	7.40	0.5181	59.26	11.12	0.5181	59.14	6.97	0.5181
MONO (K/μl)	0.49	0.15	0.51	0.33	0.7454	0.57	0.09	0.7454	0.38	0.12	0.7454	0.30	0.14	0.7454
MONO (%)	9.15	2.02	10.84	4.12	0.1955	10.66	3.30	0.1955	6.62	1.62	0.1955	6.72	2.00	0.1955
EO (K/μl)	0.10	0.02	0.09	0.06	0.9042	0.09	0.03	0.9042	0.09	0.04	0.9042	0.08	0.08	0.9042
EO (%)	1.88	0.46	1.86	0.77	0.8608	1.80	0.85	0.8608	1.48	0.30	0.8608	1.56	0.80	0.8608
BASO (K/μl)	0.03	0.06	0.00	0.00	>0.9999	0.16	0.11	>0.9999	0.03	0.08	>0.9999	0.00	0.00	>0.9999
BASO (%)	0.60	1.20	0.00	0.00	>0.9999	2.58	1.91	>0.9999	0.34	0.76	>0.9999	0.00	0.00	>0.9999

CBC: complete blood count, RBC: red blood cell, HGB: hemoglobin, HCT: hematocrit, MCV: mean corpuscular volume, MCH: mean corpuscular hemoglobin, MCHC: mean corpuscular hemoglobin concentration, RDW-CV: red cell distribution width, PLT: platelet, WBC: white blood cells, RET: reticulocyte, NEUT: neutrophil, LYMPH: lymphocyte, MONO: monocyte, EO: eosinophil, BASO: basophil.
*$P < 0.05$, **$P < 0.01$, ***$P < 0.001$, ****$P < 0.0001$.

Table 6. Clinical Chemistry Analysis at 1, 3, and 6 Months Following Subretinal Transplantation of Engineered Human Retinal Cell Grafts in Immunocompromised Rowett Nude Rats.

	Average	SD	Average	SD	*P*-value	Average	SD	*P*-value	Average	SD	*P*-value	Average	SD	*P*-value
Sex	M	M	M	M	M	M	M	M	M	M	M	M	M	M
Time point	1 M	1 M	1 M	1 M	1 M	1 M	1 M	1 M	1 M	1 M	1 M	1 M	1 M	1 M
Treatment group	Control	Control	P1	P1	Control vs P1	P2	P2	Control vs P2	P3	P3	Control vs P3	P4	P4	Control vs P4
1M Male Clinical Chemistry														
Total protein (g/dl)	6.23	0.22	6.36	0.18	0.1003	6.16	0.15	0.1003	6.05	0.45	0.1003	5.84	0.25	0.1003
Albumin (g/dl)	3.48	0.13	3.52	0.08	>0.9999	3.52	0.04	>0.9999	3.44	0.23	>0.9999	3.34	0.15	0.8395
Globulin (g/dl)	32.34	66.28	2.84	0.13	0.4945	2.64	0.13	0.4945	2.68	0.25	0.4945	2.50	0.12	0.4945
Sodium (mEq/l)	119.67	63.86	148.44	0.17	0.4896	149.30	1.73	0.4896	146.44	5.52	0.4896	145.34	3.73	0.4896
Potassium (mEq/l)	25.08	40.43	7.95	0.77	0.4215	6.38	0.50	0.4215	6.79	0.43	0.4215	7.75	0.40	0.4215
Chloride (mEq/l)	86.18	27.50	97.98	0.48	0.4259	97.66	0.61	0.4259	95.22	2.74	0.4259	96.18	2.67	0.4259
Total CO_2 (mEq/l)	34.90	13.39	33.20	4.21	0.4961	41.60	2.61	0.4961	37.80	7.33	0.4961	36.40	5.03	0.4961
Calcium (g/dl)	11.48	0.64	12.18	0.48	0.5378	11.84	0.29	0.5378	12.00	0.79	0.5378	12.18	0.41	0.5378
Glucose (mg/dl)	146.60	22.96	261.00	107.44	0.3635	209.60	52.21	0.3635	150.00	46.62	0.3635	215.80	71.21	0.3635
Alkaline phosphatase (U/l)	114.20	49.69	114.40	11.08	>0.9999	138.20	11.48	0.8531	138.40	18.72	0.8470	172.80	14.89	0.0139*
Alanine aminotransferase (U/l)	43.60	8.32	37.40	6.84	0.5813	36.00	3.16	0.5813	38.40	4.16	0.5813	36.80	3.19	0.5813
Aspartate aminotransferase (U/l)	84.25	32.53	67.00	19.30	0.4666	63.40	17.10	0.4666	69.60	18.08	0.4666	70.00	23.80	0.4666
Lactate dehydrogenase (U/l)	577.25	422.94	184.60	97.79	0.4716	147.40	41.99	0.4716	200.50	38.96	0.4716	194.60	73.53	0.4716
Total bilirubin (mg/dl)	0.15	0.06	0.14	0.05	0.6856	0.10	0.00	0.6856	0.15	0.06	0.6856	0.13	0.05	0.6856
Phosphorus (mg/dl)	10.50	4.24	9.70	0.51	0.9986	8.62	0.70	0.7255	9.95	1.10	>0.9999	11.84	0.72	0.9500
Blood urea nitrogen (mg/dl)	17.25	1.71	19.00	1.22	0.3362	17.80	3.96	0.3362	20.60	3.44	0.3362	18.40	2.41	0.3362
Creatinine (mg/dl)	14.68	32.05	0.32	0.04	0.4955	0.35	0.05	0.4955	0.28	0.03	0.4955	0.26	0.02	0.4955
Cholesterol (mg/dl)	94.25	4.35	92.20	9.68	0.1222	80.60	13.69	0.1222	93.20	12.76	0.1222	75.40	10.60	0.1222
Triglycerides (mg/dl)	143.25	28.02	151.40	39.78	>0.9999	133.40	33.16	>0.9999	197.00	28.08	0.6472	145.60	26.05	>0.9999
Creatine kinase (U/l)	245.75	166.32	187.20	158.78	0.5086	176.00	177.21	0.5086	248.20	179.76	0.5086	250.00	245.95	0.5086
Uric acid (mg/dl)	7.72	12.46	4.37	1.32	0.6941	2.41	0.93	0.6941	2.53	0.78	0.6941	3.87	0.84	0.6941
HDL (mg/dl)	27.60	11.65	28.20	1.92	0.0940	30.20	4.76	0.0940	32.00	5.20	0.0940	29.60	2.97	0.0940
LDL (9 mg/dl)	8.50	1.29	9.00	0.71	>0.9999	10.00	2.00	0.8324	8.00	1.22	>0.9999	7.00	1.87	0.8324
	Average	SD	Average	SD	*P*-value	Average	SD	*P*-value	Average	SD	*P*-value	Average	SD	*P*-value
Sex	F	F	F	F	F	F	F	F	F	F	F	F	F	F
Time point	1 M	1 M	1 M	1 M	1 M	1 M	1 M	1 M	1 M	1 M	1 M	1 M	1 M	1 M
Treatment group	Control	Control	P1	P1	Control vs P1	P2	P2	Control vs P2	P3	P3	Control vs P3	P4	P4	Control vs P4
1M Female Clinical Chemistry														
Total protein (g/dl)	6.34	0.34	6.33	0.42	0.1003	6.18	0.19	0.1003	6.08	0.23	0.1003	6.32	0.16	0.1003
Albumin (g/dl)	3.80	0.12	3.70	0.17	0.9765	3.64	0.09	0.7126	3.56	0.11	0.1906	3.64	0.15	0.7126
Globulin (g/dl)	2.54	0.23	2.70	0.37	0.4945	2.54	0.15	0.4945	2.52	0.15	0.4945	2.68	0.29	0.4945
Sodium (mEq/l)	148.44	1.28	148.44	2.29	0.4896	148.72	1.11	0.4896	142.86	3.17	0.4896	146.22	2.23	0.4896
Potassium (mEq/l)	6.05	1.30	6.80	0.90	0.4215	5.65	0.75	0.4215	6.98	0.26	0.4215	5.95	0.77	0.4215
Chloride (mEq/l)	100.04	1.47	100.28	1.10	0.4259	99.52	0.63	0.4259	95.64	3.16	0.4259	97.06	2.95	0.4259
Total CO_2 (mEq/l)	36.80	3.63	33.00	2.83	0.4961	38.80	4.21	0.4961	35.00	1.22	0.4961	35.40	4.39	0.4961
Calcium (g/dl)	11.74	0.63	11.78	0.19	0.5378	11.48	0.60	0.5378	11.72	0.81	0.5378	11.78	0.47	0.5378
Glucose (mg/dl)	251.80	105.22	250.50	100.93	0.3635	169.60	75.92	0.3635	229.00	121.74	0.3635	198.00	87.43	0.3635
Alkaline phosphatase (U/l)	119.40	11.80	106.20	22.70	0.9967	108.40	28.77	0.9992	121.80	19.61	>0.9999	143.40	25.68	0.8531
Alanine aminotransferase (U/l)	33.60	3.21	34.80	5.31	0.5813	33.40	1.95	0.5813	39.20	17.80	0.5813	37.60	4.72	0.5813
Aspartate aminotransferase (U/l)	62.60	13.50	87.75	27.93	0.4666	78.60	22.74	0.4666	123.60	129.06	0.4666	116.60	47.40	0.4666
Lactate dehydrogenase (U/l)	196.20	68.81	193.25	145.59	0.4716	166.80	77.08	0.4716	657.40	1118.08	0.4716	312.20	182.38	0.4716
Total bilirubin (mg/dl)	0.10	0.00	0.13	0.05	0.6856	0.12	0.04	0.6856	0.14	0.05	0.6856	0.14	0.05	0.6856
Phosphorus (mg/dl)	7.04	1.30	8.00	1.62	0.9965	7.50	0.81	>0.9999	10.36	0.76	0.0736	8.98	0.78	0.6899
Blood urea nitrogen (mg/dl)	17.20	1.64	19.20	2.49	0.3362	21.80	6.53	0.3362	21.60	4.39	0.3362	19.20	1.79	0.3362
Creatinine (mg/dl)	0.36	0.04	0.31	0.04	0.4955	0.36	0.02	0.4955	0.31	0.05	0.4955	0.30	0.03	0.4955
Cholesterol (mg/dl)	99.60	12.42	83.50	11.50	0.1222	96.40	7.40	0.1222	96.40	18.08	0.1222	92.80	21.95	0.1222
Triglycerides (mg/dl)	99.00	36.69	78.00	14.99	0.9982	90.20	52.44	>0.9999	116.60	18.37	0.9993	113.60	71.73	0.9998
Creatine kinase (U/l)	144.60	132.89	262.50	261.40	0.5086	266.20	163.19	0.5086	7366.20	16005.95	0.5086	557.40	445.83	0.5086
Uric acid (mg/dl)	3.03	1.49	3.54	0.53	0.6941	2.11	0.86	0.6941	3.82	1.19	0.6941	3.05	1.00	0.6941
HDL (mg/dl)	36.80	3.96	28.50	3.51	0.0940	35.60	0.89	0.0940	34.20	4.55	0.0940	32.60	5.37	0.0940
LDL (mg/dl)	6.20	0.84	6.50	0.58	>0.9999	7.40	1.52	0.9287	5.20	0.84	0.9766	6.00	1.87	>0.9999

(continued)

Table 6. (continued)

	Average	SD	Average	SD	*P*-value	Average	SD	*P*-value	Average	SD	*P*-value	Average	SD	*P*-value
Sex	M	M	M	M	M	M	M	M	M	M	M	M	M	M
Time point	3 M	3 M	3 M	3 M	3 M	3 M	3 M	3 M	3 M	3 M	3 M	3 M	3 M	3 M
Treatment group	Control	Control	P1	P1	Control vs P1	P2	P2	Control vs P2	P3	P3	Control vs P3	P4	P4	Control vs P4
3M Male Clinical Chemistry														
Total protein (g/dl)	6.10	0.27	6.12	0.08	0.7473	6.26	0.34	0.7473	6.34	0.23	0.7473	6.12	0.16	0.7473
Albumin (g/dl)	3.30	0.20	3.38	0.08	0.0768	3.44	0.11	0.0768	3.54	0.09	0.0768	3.46	0.09	0.0768
Globulin (g/dl)	2.80	0.12	2.74	0.05	0.0713	2.82	0.24	0.0713	2.80	0.16	0.0713	2.66	0.11	0.0713
Sodium (mEq/l)	148.46	1.41	143.50	2.90	0.1184	147.92	4.02	>0.9999	149.10	2.12	>0.9999	150.38	1.54	0.9755
Potassium (mEq/l)	6.63	0.32	8.86	1.29	0.0094**	8.60	1.10	0.0325*	7.47	1.02	0.8868	6.81	0.85	>0.9999
Chloride (mEq/l)	97.66	1.00	99.48	2.67	0.3386	98.86	3.35	0.3386	98.90	1.91	0.3386	99.64	0.71	0.3386
Total CO_2 (mEq/l)	36.00	4.18	30.60	4.62	0.2771	36.00	3.54	>0.9999	40.00	1.58	0.6787	32.80	3.49	0.8811
Calcium (g/dl)	11.36	0.65	11.64	0.43	0.6069	12.04	0.69	0.6069	12.00	0.68	0.6069	11.42	0.31	0.6069
Glucose (mg/dl)	194.40	37.51	189.80	59.48	0.9050	202.20	66.81	0.9050	161.20	55.65	0.9050	179.80	62.63	0.9050
Alkaline phosphatase (U/l)	117.40	12.01	128.40	12.66	0.9483	118.60	8.88	>0.9999	114.60	19.19	>0.9999	120.80	17.21	>0.9999
Alanine aminotransferase (U/l)	42.20	3.96	41.60	4.16	0.0502	34.40	3.91	0.0502	36.20	4.87	0.0502	38.40	6.50	0.0502
Aspartate aminotransferase (U/l)	58.40	4.93	106.20	83.16	0.3819	63.20	20.49	0.3819	69.20	16.75	0.3819	73.60	28.04	0.3819
Lactate dehydrogenase (U/l)	172.80	36.17	478.40	290.34	0.0682	224.40	80.79	>0.9999	186.60	78.72	>0.9999	223.80	168.08	>0.9999
Total bilirubin (mg/dl)	0.12	0.04	0.18	0.04	0.3867	0.18	0.04	0.3867	0.18	0.04	0.3867	0.14	0.05	0.9985
Phosphorus (mg/dl)	7.86	0.59	9.28	1.19	0.2694	9.98	0.44	0.0146*	9.48	0.69	0.1332	8.50	1.08	0.9752
Blood urea nitrogen (mg/dl)	19.00	3.08	19.60	2.41	0.1022	21.20	5.07	0.1022	19.40	2.41	0.1022	23.60	5.46	0.1022
Creatinine (mg/dl)	0.30	0.05	0.31	0.05	0.4783	0.29	0.06	0.4783	0.33	0.03	0.4783	0.32	0.07	0.4783
Cholesterol (mg/dl)	90.40	7.57	90.00	8.80	>0.9999	85.40	8.73	0.9977	94.80	6.57	0.9991	91.40	6.54	>0.9999
Triglycerides (mg/dl)	134.00	19.70	143.80	35.73	>0.9999	139.00	19.14	>0.9999	177.20	39.12	0.5272	120.80	18.91	0.9997
Creatine kinase (U/l)	128.80	51.17	547.60	687.54	0.4554	208.80	188.33	0.4554	198.80	143.12	0.4554	295.80	377.23	0.4554
Uric acid (mg/dl)	2.10	0.75	3.49	0.93	0.1908	4.21	1.06	0.1908	3.21	1.24	0.1908	2.71	1.00	0.1908
HDL (mg/dl)	31.80	2.77	31.20	1.79	>0.9999	30.20	2.17	0.9930	29.40	2.41	0.9073	32.20	1.48	>0.9999
LDL (mg/dl)	8.20	1.48	8.40	1.52	>0.9999	6.80	1.48	0.6833	9.60	1.52	0.6833	9.40	1.14	0.8358
	Average	SD	Average	SD	*P*-value	Average	SD	*P*-value	Average	SD	*P*-value	Average	SD	*P*-value
Sex	F	F	F	F	F	F	F	F	F	F	F	F	F	F
Time point	3 M	3 M	3 M	3 M	3 M	3 M	3 M	3 M	3 M	3 M	3 M	3 M	3 M	3 M
Treatment group	Control	Control	P1	P1	Control vs P1	P2	P2	Control vs P2	P3	P3	Control vs P3	P4	P4	Control vs P4
3M Female Clinical Chemistry														
Total protein (g/dl)	6.33	0.28	6.28	0.31	0.7473	6.46	0.40	0.7473	6.36	0.74	0.7473	6.08	0.38	0.7473
Albumin (g/dl)	3.66	0.13	3.62	0.19	0.0768	3.64	0.32	0.0768	3.72	0.45	0.0768	3.60	0.20	0.0768
Globulin (g/dl)	2.65	0.17	2.66	0.15	0.0713	2.82	0.11	0.0713	2.64	0.30	0.0713	2.48	0.18	0.0713
Sodium (mEq/l)	148.98	2.42	146.20	2.03	0.8062	147.62	2.19	0.9979	145.54	4.31	0.5619	150.16	1.65	0.9993
Potassium (mEq/l)	6.00	0.61	6.59	1.34	0.9871	6.23	0.59	>0.9999	6.92	0.54	0.8169	5.63	0.54	0.9996
Chloride (mEq/l)	97.92	1.26	97.62	2.52	0.3386	100.88	1.83	0.3386	98.42	3.76	0.3386	100.28	1.82	0.3386
Total CO_2 (mEq/l)	33.20	3.70	32.20	2.49	>0.9999	35.40	2.70	0.9879	35.20	3.56	0.9939	31.80	2.59	0.9996
Calcium (g/dl)	11.78	0.83	11.52	0.77	0.6069	11.58	0.47	0.6069	12.04	0.72	0.6069	11.56	0.62	0.6069
Glucose (mg/dl)	226.40	59.54	232.40	105.76	0.9050	208.60	84.38	0.9050	206.40	54.56	0.9050	209.80	96.24	0.9050
Alkaline phosphatase (U/l)	112.00	9.25	96.00	6.75	0.6764	116.20	18.77	>0.9999	94.00	12.04	0.5222	96.80	10.89	0.7349
Alanine aminotransferase (U/l)	38.60	3.13	37.60	5.32	0.0502	33.00	5.39	0.0502	36.00	9.08	0.0502	31.80	3.11	0.0502
Aspartate aminotransferase (U/l)	60.20	5.89	56.00	7.52	0.3819	108.40	74.38	0.3819	74.00	23.07	0.3819	81.80	36.72	0.3819
Lactate dehydrogenase (U/l)	132.20	57.85	173.20	74.81	>0.9999	306.60	258.59	0.7087	177.40	89.83	>0.9999	181.40	122.08	>0.9999
Total bilirubin (mg/dl)	0.10	0.00	0.10	0.00	>0.9999	0.12	0.04	0.9991	0.16	0.05	0.4687	0.10	0.00	>0.9999
Phosphorus (mg/dl)	7.30	0.69	7.48	1.58	>0.9999	7.28	0.67	>0.9999	8.52	0.41	0.4735	8.00	0.72	0.9564
Blood urea nitrogen (mg/dl)	18.00	1.22	16.60	2.07	0.1022	19.60	0.55	0.1022	20.00	3.81	0.1022	18.40	1.67	0.1022
Creatinine (mg/dl)	0.31	0.04	0.32	0.06	0.4783	0.34	0.05	0.4783	0.37	0.08	0.4783	0.29	0.03	0.4783
Cholesterol (mg/dl)	107.20	14.69	98.00	9.35	0.8751	90.60	10.90	0.1902	86.20	12.19	0.0364*	81.60	6.73	0.0045***
Triglycerides (mg/dl)	80.00	23.59	101.80	24.67	0.9901	93.60	27.75	0.9997	145.20	63.01	0.1101	92.60	21.52	0.9999
Creatine kinase (U/l)	125.60	22.61	100.40	41.98	0.4554	525.40	659.16	0.4554	226.80	210.10	0.4554	283.40	289.36	0.4554
Uric acid (mg/dl)	2.45	1.22	2.68	1.69	0.1908	2.87	1.03	0.1908	3.40	0.53	0.1908	2.85	1.10	0.1908
HDL (mg/dl)	39.40	4.51	36.60	2.07	0.8007	34.00	2.92	0.0654	30.80	2.59	0.0003***	31.20	2.49	0.0006***
LDL (mg/dl)	5.60	0.89	5.00	1.00	0.9981	4.40	0.55	0.8358	5.40	0.89	>0.9999	5.80	0.84	>0.9999

(continued)

Table 6. (continued)

	Average	SD	Average	SD	*P*-value	Average	SD	*P*-value	Average	SD	*P*-value	Average	SD	*P*-value
Sex	M	M	M	M	M	M	M	M	M	M	M	M	M	M
Time point	6 M	6 M	6 M	6 M	6 M	6 M	6 M	6 M	6 M	6 M	6 M	6 M	6 M	6 M
Treatment group	Control	Control	P1	P1	Control vs P1	P2	P2	Control vs P2	P3	P3	Control vs P3	P4	P4	Control vs P4
6M Male Clinical Chemistry														
Total protein (g/dl)	5.94	0.33	6.10	0.27	0.9999	6.28	0.33	0.9533	6.03	0.30	>0.9999	6.24	0.28	0.9810
Albumin (g/dl)	3.32	0.08	3.27	0.29	>0.9999	3.48	0.13	0.9925	3.30	0.07	>0.9999	3.46	0.09	0.9976
Globulin (g/dl)	2.62	0.25	2.83	0.14	0.4196	2.80	0.21	0.4196	2.73	0.26	>0.9999	2.78	0.23	0.4196
Sodium (mEq/l)	149.30	1.81	149.88	2.11	>0.9999	152.26	3.21	0.6615	150.38	2.22	0.9998	146.94	1.36	0.8889
Potassium (mEq/l)	7.32	1.47	6.85	1.17	0.1270	7.40	0.92	0.1270	6.85	0.72	0.1270	7.66	0.35	0.1270
Chloride (mEq/l)	97.96	1.09	98.33	1.09	>0.9999	100.02	1.52	0.7336	99.76	1.74	0.8645	97.32	1.59	>0.9999
Total CO_2 (mEq/l)	39.60	2.79	39.83	3.19	>0.9999	37.60	4.28	0.9991	38.00	3.16	0.9999	34.40	0.89	0.5104
Calcium (g/dl)	11.48	0.41	11.27	0.28	>0.9999	11.84	0.54	0.9940	11.20	0.43	0.9993	12.00	0.47	0.9125
Glucose (mg/dl)	188.20	80.55	165.00	47.14	>0.9999	162.20	45.12	>0.9999	121.80	36.38	0.8745	250.40	92.80	0.9146
Alkaline phosphatase (U/l)	120.00	15.36	125.00	10.86	>0.9999	104.40	25.09	0.9421	98.80	12.83	0.6944	102.60	13.74	0.8863
Alanine aminotransferase (U/l)	45.00	13.98	36.17	4.17	0.0789	32.60	2.07	0.0789	31.80	2.59	0.0789	35.00	3.39	0.0789
Aspartate aminotransferase (U/l)	71.80	26.89	57.83	10.87	0.2096	64.80	10.43	0.2096	58.40	13.20	0.2096	62.40	18.23	0.2096
Lactate dehydrogenase (U/l)	208.20	83.48	127.00	56.28	0.8082	168.60	41.28	0.8082	176.50	73.85	0.8082	170.00	81.66	0.8082
Total bilirubin (mg/dl)	0.10	0.00	0.10	0.00	0.3665	0.14	0.05	0.3665	0.15	0.06	0.3665	0.16	0.05	0.3665
Phosphorus (mg/dl)	8.24	0.86	7.62	1.10	0.0598	9.00	1.92	0.0598	7.16	3.02	0.0598	8.94	0.55	0.0598
Blood urea nitrogen (mg/dl)	18.80	1.48	17.67	2.34	0.9987	18.60	1.67	>0.9999	15.80	2.17	0.4837	19.40	2.30	>0.9999
Creatinine (mg/dl)	0.28	0.03	0.29	0.03	>0.9999	0.33	0.04	0.6347	0.28	0.04	>0.9999	0.40	0.06	0.0002***
Cholesterol (mg/dl)	95.60	10.78	95.83	10.98	>0.9999	108.80	16.21	0.9725	97.60	9.15	>0.9999	103.80	20.28	0.9995
Triglycerides (mg/dl)	117.20	15.74	147.67	56.20	0.0812	110.00	25.70	0.0812	140.25	19.29	0.0812	149.00	25.23	0.0812
Creatine kinase (U/l)	193.60	150.37	128.83	81.63	0.3430	196.80	90.60	0.3430	165.00	120.22	0.3430	167.80	130.01	0.3430
Uric acid (mg/dl)	2.98	1.13	2.29	1.16	0.0978	3.35	1.22	0.0978	1.97	0.92	0.0978	3.95	1.13	0.0978
HDL (mg/dl)	33.60	2.70	29.83	4.26	0.9503	30.80	4.21	0.9964	27.80	2.49	0.6152	31.00	4.06	0.9981
LDL (9 mg/dl)	9.00	0.71	9.50	1.05	>0.9999	10.80	1.10	0.6028	9.20	0.84	>0.9999	8.80	1.30	>0.9999
	Average	SD	Average	SD	*P*-value	Average	SD	*P*-value	Average	SD	*P*-value	Average	SD	*P*-value
Sex	F	F	F	F	F	F	F	F	F	F	F	F	F	F
Time point	6 M	6 M	6 M	6 M	6 M	6 M	6 M	6 M	6 M	6 M	6 M	6 M	6 M	6 M
Treatment group	Control	Control	P1	P1	Control vs P1	P2	P2	Control vs P2	P3	P3	Control vs P3	P4	P4	Control vs P4
6M Female Clinical Chemistry														
Total protein (g/dl)	6.85	0.58	6.42	0.35	0.8683	6.76	0.53	>0.9999	6.33	0.19	0.7165	6.63	0.33	0.9994
Albumin (g/dl)	3.95	0.30	3.76	0.25	0.9818	3.98	0.32	>0.9999	3.74	0.13	0.9622	3.94	0.26	>0.9999
Globulin (g/dl)	2.90	0.42	2.66	0.13	0.4196	2.78	0.24	0.4196	2.55	0.13	0.7377	2.70	0.32	0.4196
Sodium (mEq/l)	146.58	1.49	147.60	3.20	>0.9999	149.26	1.18	0.8360	149.48	2.09	0.7577	147.90	2.47	0.9992
Potassium (mEq/l)	6.80	1.14	5.89	0.56	0.1270	6.07	0.11	0.1270	5.90	0.53	0.1270	6.00	0.85	0.1270
Chloride (mEq/l)	97.33	2.67	97.48	1.92	>0.9999	99.20	0.89	0.8776	99.42	2.16	0.7807	98.52	1.45	0.9952
Total CO_2 (mEq/l)	31.00	4.24	36.40	4.83	0.5423	36.40	2.19	0.5423	33.80	1.92	0.9902	32.60	3.36	>0.9999
Calcium (g/dl)	12.35	0.87	11.58	0.31	0.5662	12.02	0.43	0.9983	11.74	0.36	0.8440	11.96	0.82	0.9929
Glucose (mg/dl)	274.00	82.03	165.40	62.91	0.3272	216.20	23.76	0.9643	229.50	31.17	0.9970	186.80	87.54	0.6510
Alkaline phosphatase (U/l)	93.25	16.68	97.60	16.47	>0.9999	122.60	19.65	0.3063	100.60	8.38	>0.9999	88.80	9.81	>0.9999
Alanine aminotransferase (U/l)	42.00	11.22	57.40	35.22	0.0789	57.00	18.53	0.0789	37.00	6.56	0.0789	36.80	3.56	0.0789
Aspartate aminotransferase (U/l)	69.00	24.12	106.60	55.83	0.2096	85.40	23.89	0.2096	69.20	18.54	0.2096	76.00	29.92	0.2096
Lactate dehydrogenase (U/l)	145.00	29.74	217.00	90.22	0.8082	134.60	77.53	0.8082	139.50	15.86	0.8082	157.00	92.86	0.8082
Total bilirubin (mg/dl)	0.13	0.05	0.12	0.04	0.3665	0.14	0.05	0.3665	0.13	0.05	0.3665	0.15	0.07	0.3665
Phosphorus (mg/dl)	7.03	1.34	7.40	0.93	0.0598	6.50	0.42	0.0598	6.43	0.64	0.0598	7.20	1.28	0.0598
Blood urea nitrogen (mg/dl)	17.50	3.11	17.00	2.35	>0.9999	20.40	2.30	0.6214	17.60	2.07	>0.9999	16.80	1.92	>0.9999
Creatinine (mg/dl)	0.32	0.05	0.28	0.02	0.9544	0.37	0.04	0.8049	0.32	0.04	>0.9999	0.31	0.04	>0.9999
Cholesterol (mg/dl)	119.25	15.13	120.60	20.21	>0.9999	105.60	17.21	0.9772	104.40	7.06	0.9582	103.60	16.65	0.9406
Triglycerides (mg/dl)	118.25	59.09	104.20	15.99	0.0812	151.40	69.57	0.0812	120.75	21.53	0.0812	75.50	5.51	0.0812
Creatine kinase (U/l)	151.25	116.93	300.00	308.05	0.3430	106.00	76.84	0.3430	100.60	46.52	0.3430	259.40	222.82	0.3430
Uric acid (mg/dl)	3.88	1.73	2.33	0.96	0.0978	2.53	0.46	0.0978	2.48	0.67	0.0978	2.09	0.19	0.0978
HDL (mg/dl)	38.50	5.20	38.40	3.29	>0.9999	36.20	5.81	0.9996	35.40	1.52	0.9948	35.00	4.36	0.9862
LDL (mg/dl)	5.50	1.00	5.60	0.55	>0.9999	5.60	0.89	>0.9999	5.75	1.26	>0.9999	4.40	0.55	0.9836

HDL: high-density lipoprotein; LDL: low-density lipoprotein.
*$P < 0.05$, **$P < 0.01$, ***$P < 0.001$.

Table 7. Summary of Histopathology Findings (Gross) at 1, 3, and 6 Months Following Subretinal Transplantation of Engineered Human Retinal Progenitor Cell Grafts in Immunocompromised Rowett Nude Rats.

	Control		P1		P2		P3		P4	
	M	F	M	F	M	F	M	F	M	F
1 Month										
Kidney										
Hydronephrosis in left kidney	1/5	—	—	—	—	—	—	—	—	—
Adipose tissue										
Subcutaneous red discoloration at the inguinal region	—	—	—	—	1/5	—	—	—	—	—
Mesentery										
Mesenteric lymph node appeared somewhat large	—	—	—	—	—	—	—	—	—	1/5
3 Months										
Kidney										
Hydronephrosis in right kidney	1/5	—	—	—	—	—	—	—	—	—
Mildly dilated renal pelvis in left kidney	1/5	—	1/5	—	—	—	—	—	—	—
Reproductive organs										
Left testicular hypoplasia	—	N/A	1/5	N/A	—	N/A	—	N/A	—	N/A
Skin										
Hair loss due to barbering	—	—	—	—	—	—	—	—	—	1/5
6 Months										
Kidney										
No left kidney	—	1/4	—	—	—	—	—	—	1/5	—
Enlarged right kidney	—	—	—	—	—	—	—	—	1/5	—
Reproductive										
Left ovary greatly enlarged/cystic	N/A	1/4	N/A	—	N/A	—	N/A	—	N/A	—
Left uterine horn dilated	N/A	1/4	N/A	—	N/A	—	N/A	—	N/A	—
Enlarged uterus	N/A	—	N/A	—	N/A	—	N/A	—	N/A	1/5
No left seminal vesicle	—	N/A	—	N/A	—	N/A	—	N/A	1/5	N/A
Small left testicle	—	N/A	—	N/A	—	N/A	—	N/A	1/5	N/A
Mesentery										
Large mesenteric lymph node(s)	—	—	—	—	—	—	—	1/5	—	—

(—): not observed in any animals; N/A: not applicable.

Table 8. Animal Organ Weights at 1, 3, and 6 Months Following Subretinal Transplantation of Engineered Human Retinal Progenitor Cell Grafts in Immunocompromised Rowett Nude Rats.

	Average	SD	Average	SD	*P*-value	Average	SD	*P*-value	Average	SD	*P*-value	Average	SD	*P*-value
Sex	M	M	M	M	M	M	M	M	M	M	M	M	M	M
Time point	1 M	1 M	1 M	1 M	1 M	1 M	1 M	1 M	1 M	1 M	1 M	1 M	1 M	1 M
Treatment group	Control	Control	P1	P1	Control vs P1	P2	P2	Control vs P2	P3	P3	Control vs P3	P4	P4	Control vs P4
1M Male Organ Weights														
Heart (g)	1.08	0.06	1.63	1.12	0.3402	1.12	0.11	>0.9999	1.12	0.12	>0.9999	1.01	0.08	>0.9999
Thymus (g)	0.11	0.05	0.12	0.04	>0.9999	0.13	0.06	>0.9999	0.19	0.15	0.6963	0.12	0.03	>0.9999
Lungs with Trachea (g)	2.41	0.30	2.52	0.39	>0.9999	2.50	0.62	>0.9999	3.03	0.50	0.4813	2.20	0.52	0.9978
Pancreas (g)	1.34	0.22	1.25	0.15	0.9977	1.21	0.26	0.9599	1.39	0.16	>0.9999	1.37	0.14	>0.9999
Spleen (g)	0.72	0.02	0.66	0.07	>0.9999	0.67	0.10	>0.9999	0.66	0.05	>0.9999	0.72	0.20	>0.9999
Kidneys (g)	3.07	0.28	2.69	0.37	0.4359	3.03	0.28	>0.9999	2.96	0.29	0.9994	2.66	0.36	0.3115
Liver (g)	14.23	1.60	12.71	1.20	>0.9999	13.31	0.64	>0.9999	14.69	1.92	>0.9999	12.40	1.52	>0.9999
Brain (g)	1.97	0.07	1.90	0.05	0.9887	2.01	0.07	>0.9999	1.98	0.12	>0.9999	2.07	0.15	0.8585
	Average	SD	Average	SD	*P*-value	Average	SD	*P*-value	Average	SD	*P*-value	Average	SD	*P*-value
Sex	F	F	F	F	F	F	F	F	F	F	F	F	F	F
Time point	1 M	1 M	1 M	1 M	1 M	1 M	1 M	1 M	1 M	1 M	1 M	1 M	1 M	1 M
Treatment group	Control	Control	P1	P1	Control vs P1	P2	P2	Control vs P2	P3	P3	Control vs P3	P4	P4	Control vs P4
1M Female Organ Weight														
Heart (g)	0.89	0.06	0.82	0.03	>0.9999	0.77	0.06	>0.9999	0.89	0.09	>0.9999	0.87	0.06	>0.9999
Thymus (g)	0.08	0.02	0.09	0.03	>0.9999	0.10	0.05	0.9998	0.34	0.10	<0.0001****	0.10	0.06	>0.9999
Lungs with Trachea (g)	2.23	0.40	1.94	0.28	0.9789	1.94	0.25	0.9824	2.00	0.45	0.9967	2.03	0.35	0.9988
Pancreas (g)	1.09	0.10	1.01	0.05	0.9985	0.88	0.14	0.5948	0.91	0.21	0.7947	1.30	0.19	0.6904
Spleen (g)	0.51	0.03	0.49	0.07	>0.9999	0.50	0.03	>0.9999	0.55	0.08	>0.9999	0.54	0.08	>0.9999
Kidneys (g)	1.82	0.16	1.71	0.19	0.9993	1.86	0.11	>0.9999	1.94	0.24	0.9991	1.86	0.24	>0.9999
Liver (g)	8.75	0.66	7.67	0.74	>0.9999	8.35	0.51	>0.9999	8.96	0.29	>0.9999	10.01	2.23	>0.9999
Brain (g)	1.74	0.18	1.76	0.07	>0.9999	1.79	0.05	0.9993	1.80	0.08	0.9973	1.83	0.12	0.9417
	Average	SD	Average	SD	*P*-value	Average	SD	*P*-value	Average	SD	*P*-value	Average	SD	*P*-value
Sex	M	M	M	M	M	M	M	M	M	M	M	M	M	M
Time point	3 M	3 M	3 M	3 M	3 M	3 M	3 M	3 M	3 M	3 M	3 M	3 M	3 M	3 M
Treatment group	Control	Control	P1	P1	Control vs P1	P2	P2	Control vs P2	P3	P3	Control vs P3	P4	P4	Control vs P4
3M Male Organ Weights														
Heart (g)	1.18	0.12	1.17	0.15	>0.9999	1.23	0.10	0.9996	1.12	0.17	0.9968	1.20	0.18	>0.9999
Thymus (g)	0.15	0.05	0.17	0.11	0.7921	0.10	0.03	0.7921	0.12	0.09	0.7921	0.13	0.04	0.7921
Lungs with Trachea (g)	2.11	0.69	2.28	0.48	0.9996	2.91	0.67	0.1027	2.98	0.57	0.0586	2.34	0.22	0.9967
Pancreas (g)	0.93	0.16	1.00	0.22	>0.9999	1.46	0.32	0.0730	1.52	0.23	0.0313*	1.10	0.22	0.9890
Spleen (g)	0.68	0.07	0.70	0.03	>0.9999	0.87	0.22	0.2132	0.76	0.08	0.9712	0.74	0.06	0.9976
Kidneys (g)	3.14	0.32	3.29	0.29	0.9880	3.36	0.31	0.8921	2.91	0.34	0.8476	2.82	0.14	0.5067
Liver (g)	13.84	1.59	15.35	1.98	0.7591	14.89	1.07	0.9665	14.44	2.61	0.9994	13.02	0.89	0.9931
Brain (g)	2.00	0.09	2.42	0.95	0.4766	2.07	0.03	>0.9999	2.02	0.06	>0.9999	2.01	0.06	>0.9999

(continued)

Table 8. (continued)

	Average	SD	Average	SD	*P*-value	Average	SD	*P*-value	Average	SD	*P*-value	Average	SD	*P*-value
Sex	F	F	F	F	F	F	F	F	F	F	F	F	F	F
Time point	3 M	3 M	3 M	3 M	3 M	3 M	3 M	3 M	3 M	3 M	3 M	3 M	3 M	3 M
Treatment group	Control	Control	P1	P1	Control vs P1	P2	P2	Control vs P2	P3	P3	Control vs P3	P4	P4	Control vs P4
3M Female Organ Weights														
Heart (g)	0.85	0.06	0.86	0.06	>0.9999	0.88	0.05	>0.9999	0.86	0.14	>0.9999	0.75	0.09	0.9439
Thymus (g)	0.13	0.06	0.11	0.05	0.7921	0.10	0.02	0.7921	0.26	0.37	0.7921	0.25	0.36	0.7921
Lungs with Trachea (g)	1.71	0.18	1.50	0.26	0.9987	1.94	0.22	0.9965	2.31	0.22	0.4297	2.02	0.16	0.9696
Pancreas (g)	1.02	0.26	0.80	0.18	0.9449	1.20	0.44	0.9842	1.20	0.29	0.9855	1.25	0.19	0.9396
Spleen (g)	0.55	0.04	0.54	0.02	>0.9999	0.50	0.23	0.9996	0.56	0.09	>0.9999	0.54	0.05	>0.9999
Kidneys (g)	1.96	0.13	1.94	0.16	>0.9999	1.75	0.20	0.9017	1.90	0.13	>0.9999	1.79	0.16	0.9722
Liver (g)	8.92	0.89	9.42	0.40	>0.9999	8.35	0.90	0.9970	8.69	0.76	>0.9999	8.38	1.00	>0.9999
Brain (g)	1.86	0.06	1.87	0.08	>0.9999	1.65	0.11	0.9848	1.84	0.08	>0.9999	1.77	0.06	>0.9999
	Average	SD	Average	SD	*P*-value	Average	SD	*P*-value	Average	SD	*P*-value	Average	SD	*P*-value
Sex	M	M	M	M	M	M	M	M	M	M	M	M	M	M
Time point	6 M	6 M	6 M	6 M	6 M	6 M	6 M	6 M	6 M	6 M	6 M	6 M	6 M	6 M
Treatment group	Control	Control	P1	P1	Control vs P1	P2	P2	Control vs P2	P3	P3	Control vs P3	P4	P4	Control vs P4
6M Male Organ Weights														
Heart (g)	1.22	0.10	1.34	0.13	0.9877	1.24	0.08	>0.9999	1.35	0.16	0.9865	1.24	0.08	>0.9999
Thymus (g)	0.30	0.35	0.15	0.04	0.6159	0.29	0.37	0.6159	0.10	0.08	0.6159	0.16	0.05	0.6159
Lungs with Trachea (g)	2.84	0.47	2.86	0.17	>0.9999	3.50	0.71	0.4355	2.90	0.32	>0.9999	3.04	0.68	0.9999
Pancreas (g)	1.49	0.19	1.37	0.28	0.9999	1.40	0.26	>0.9999	1.25	0.11	0.9484	1.20	0.23	0.8135
Spleen (g)	0.78	0.06	0.86	0.15	0.9630	0.84	0.08	0.9974	0.82	0.04	>0.9999	0.79	0.09	>0.9999
Kidneys (g)	3.47	0.43	3.69	0.38	0.9976	3.34	0.22	>0.9999	3.15	0.24	0.9543	3.05	0.29	0.7967
Liver (g)	16.54	2.83	16.86	1.81	>0.9999	13.69	0.94	>0.9999	13.89	1.00	>0.9999	14.35	1.74	>0.9999
Brain (g)	2.08	0.14	2.05	0.05	>0.9999	1.98	0.09	0.8105	2.10	0.07	>0.9999	2.03	0.08	0.9996
	Average	SD	Average	SD	*P*-value	Average	SD	*P*-value	Average	SD	*P*-value	Average	SD	*P*-value
Sex	F	F	F	F	F	F	F	F	F	F	F	F	F	F
Time point	6 M	6 M	6 M	6 M	6 M	6 M	6 M	6 M	6 M	6 M	6 M	6 M	6 M	6 M
Treatment group	Control	Control	P1	P1	Control vs P1	P2	P2	Control vs P2	P3	P3	Control vs P3	P4	P4	Control vs P4
6M Female Organ Weights														
Heart (g)	0.92	0.07	0.96	0.18	>0.9999	1.02	0.04	0.9989	0.91	0.07	>0.9999	0.92	0.07	0.9141
Thymus (g)	0.16	0.08	0.27	0.29	0.6159	0.18	0.03	0.6159	0.10	0.05	0.6159	0.11	0.06	0.6159
Lungs with Trachea (g)	2.30	0.32	2.31	0.47	>0.9999	2.22	0.14	>0.9999	1.95	0.31	0.9858	2.28	0.47	>0.9999
Pancreas (g)	1.13	0.27	1.05	0.25	>0.9999	1.10	0.11	>0.9999	0.90	0.15	0.9611	1.07	0.28	>0.9999
Spleen (g)	0.52	0.09	0.61	0.04	0.9667	0.58	0.12	0.9992	0.55	0.06	>0.9999	0.61	0.09	0.9683
Kidneys (g)	2.01	0.30	2.27	0.23	0.9945	1.83	0.10	0.9999	1.86	0.11	>0.9999	2.25	0.69	0.9977
Liver (g)	9.33	1.08	10.27	1.15	>0.9999	9.14	0.51	>0.9999	8.36	0.40	>0.9999	8.48	1.03	>0.9999
Brain (g)	1.88	0.06	1.88	0.05	>0.9999	1.86	0.06	>0.9999	1.84	0.05	>0.9999	1.87	0.09	>0.9999

Table 9. Summary of Histopathology Findings (Microscopic) at 1, 3, and 6 Months Following Subretinal Transplantation of Engineered Human Retinal Progenitor Cell Grafts in Immunocompromised Rowett Nude Rats.

	Control		P1		P2		P3		P4	
	M	F	M	F	M	F	M	F	M	F
1 Month										
Head w/ eye, salivary gland, Harderian gland, optic nerve, olfactory bulb, nose, mouth										
Scattered lymphocytes and plasma cells in the parotid salivary glands	3/5	2/5	—	—	4/5	3/5	2/5	2/5	1/5	—
Moderate numbers of lymphocytes and fewer plasma cells surrounding some sebaceous glands in the eyelid	1/5	—	—	—	—	—	—	—	—	—
Embedded hairs in the oral epithelium with moderate numbers of neutrophils and cellular debris	—	—	—	—	1/5	—	—	—	—	—
Implant present within retina with locally extensive thinning of all retinal layers at the implant site	—	—	—	—	1/5	—	—	—	—	—
Implant visible within the retina and located between the inner plexiform and inner nuclear layers	—	—	—	—	—	—	1/5	—	—	—
Scattered free hairs and refractile material (likely talc) surrounded by many macrophages and fewer multinucleated giant cells within the conjunctiva	—	—	—	—	—	—	—	1/5	—	—
Implant on top of retina	—	—	—	—	—	—	—	—	1/5	—
Unilateral retinal detachment with subretinal accumulation of numerous neutrophils and fibrin	—	—	—	—	—	—	—	—	—	1/5
Multifocal to coalescing infiltrates of lymphocytes within the Harderian gland	—	—	—	—	—	—	—	—	—	1/5
Lungs										
Airways surrounded by low to moderate number of lymphocytes and plasma cells and cellular debris	—	—	—	—	1/5	2/5	—	—	—	—
Pancreas										
A single pancreatic duct surrounded by a moderate number of macrophages and lymphocytes	—	—	—	—	—	—	1/5	1/5	—	—
Multifocal, variably sized accumulations of lymphocytes, macrophages around pancreatic ducts, vessels and around and within islets	—	—	—	—	—	—	—	1/5	—	—
White adipose tissue										
Low numbers of lymphocytes, plasma cells and fewer macrophages and mast cells scattered in the peripancreatic adipose tissue	1/5	—	—	—	1/5	—	1/5	2/5	—	—
Subcutaneous hemangioma	—	—	—	—	1/5	—	—	—	—	—
Stomach										
Squamous cyst	—	—	—	—	—	—	—	—	1/5	—
Spleen										
On the splenic capsule there is a locally extensive region of capsular fibrosis	—	—	—	—	—	—	—	—	—	1/5
Thyroid gland										
Multifocal coalescing lymphocytes and plasma cells, obscuring normal colloid	—	—	1/5	—	—	—	—	—	—	—
Kidney										
Moderate dilation of the renal pelvis	1/5	—	1/5	—	—	—	3/5	—	1/5	—
Large medullary cyst	1/5	—	—	—	1/5	—	—	—	—	—
Scattered mineralized renal tubules							—	3/5	—	3/5
Heart										
A single focus of low number of lymphocytes in the myocardium of the interventricular septum	—	1/5	—	—	—	—	—	—	—	—
3 Months										
Adrenal gland										
Focus of vacuolar change within the cortex	—	—	—	—	—	2/5	—	—	—	—
Brain										
Small focus of hemorrhage within the brainstem	—	—	1/5	—	—	—	—	—	—	—
Head w/back of eye salivary gland, Harderian gland, optic nerve, olfactory bulb, nose, mouth										
Scattered lymphocytes and plasma cells within the Harderian glands	2/5	1/5	1/5	2/5	1/5	—	—	—	—	—
Scattered lymphocytes and plasma cells in parotid salivary glands	2/5	4/5	1/5	3/5	2/5	5/5	3/5	2/5	—	—
Small focus of neutrophils with fewer macrophages in the sub-epithelium connective tissue adjacent to molar tooth	—	—	—	—	—	1/5	—	—	—	—
Implant located within the sclera, deep to the retina.	—	—	—	1/5	—	—	—	—	—	—
A single unilateral focus of inflammation (neutrophils and macrophages) within the eyelid around vacuolated material (likely sebaceous gland secretions)	—	—	1/5	—	—	—	—	—	—	—
Bands of collagen surrounding the implant	—	—	—	—	1/5	—	—	—	—	—
Fibrous connective tissue surround the implant; a small focus of woven bone (most likely osseus metaplasia) is under the implant, along with scattered multinucleated giant cells	—	—	—	—	1/5	—	—	—	—	—
Free blood adjacent to implant which is surrounded by fibrous connective tissue and localized retinal disorganization	—	—	—	—	1/5	—	—	—	—	—
Small numbers of lymphocytes and plasma cells with fewer neutrophils located at the sclera adjacent to the cornea	—	—	—	—	—	1/5	—	—	—	—
Dysplastic retina	—	—	—	—	—	1/5	—	—	—	—
Cataract (outer segments) and partial retinal adherence to the iris	—	—	—	—	—	1/5	—	—	—	—

(continued)

Table 9. (continued)

	Control		P1		P2		P3		P4	
	M	F	M	F	M	F	M	F	M	F
Heart										
Small focus of lymphocytes and fewer plasma cells on the epicardial surface	—	—	—	1/5	—	—	—	—	—	—
Within the interventricular septum there are rare, multifocal and small accumulations of lymphocytes and plasma cells with rare eosinophils	—	—	—	—	—	—	1/5	1/5	—	—
Kidney										
Mineralized renal tubules	—	—	—	1/5	2/5	—	—	—	—	—
Mild to moderate dilation of renal pelvis	—	—	—	—	2/5	—	1/5	—	—	—
Foci of lymphocytes, plasma cells and macrophages in the subepithelial connective tissue of the renal pelvis which extend rarely into the medulla and cortex	—	—	—	—	1/5	1/5	—	—	—	—
Scattered degenerate neutrophils in the pelvic space	—	—	—	—	—	1/5	—	—	—	—
Liver										
Mild microvesicular hepatocellular vacuolation in the centrilobular zone of hepatocytes (likely glycogen)	—	—	2/5	2/5	—	—	1/5	—	—	—
Pancreas										
Rare foci of lymphocytes and plasma cells adjacent to islets	—	—	—	—	—	1/5	—	—	—	—
Reproductive Organs										
Multifocal testicular degeneration	—	N/A	—	N/A	—	N/A	1/5	N/A	—	N/A
Thyroid										
Small focus of lymphocytes and plasma cells along periphery	—	—	—	1/5	—	—	—	—	—	—
Trachea										
Multifocal accumulations of lymphocytes and plasma cells in the subepithelial connective tissue	—	—	—	—	—	—	1/5	—	—	—
White adipose tissue										
Within the peripancreatic fat there are scattered low numbers of lymphocytes, plasma cell and fewer macrophages and mast cells	—	—	—	—	1/5	—	—	—	—	—
6 Months										
Brain										
Scattered, multifocal neurons within the brainstem have cytoplasmic vacuolation	—	—	—	—	—	1/5	—	—	—	—
Head w/ sinus, nose, mouth (teeth, tongue, oral cavity, nasal epithelium) and base of skull										
Within the ethmoids, there is mucus and neutrophils	—	—	—	—	—	1/5	1/5	—	—	—
Head w/back of eye salivary gland, Harderian gland, optic nerve, olfactory bulb, nose, mouth										
Scattered lymphocytes and plasma cells within the Harderian glands	1/5	—	—	1/5	—	—	—	—	—	2/5
Scattered lymphocytes and plasma cells in the parotid salivary glands	3/5	3/4	—	1/5	—	—	—	—	2/5	4/5
Rare, scattered lymphocytes around salivary ducts in tongue	—	1/4	—	—	—	—	—	—	—	—
The right eye has diffuse retinal detachment with subretinal exudate	—	—	—	—	—	—	—	—	—	1/5
Kidney										
Mineralized renal tubules	—	1/4	—	—	—	—	—	—	—	1/5
Mild to moderate dilation of renal pelvis	—	—	1/6	—	—	—	—	—	1/5	
Small number of neutrophils with the renal pelvis	—	—	—	—	—	—	—	—	—	1/5
Lungs										
Multifocal small foci where foamy macrophages fill small alveolar spaces	—	—	—	—	1/5	—	—	—	—	—
Pancreas										
Small, single focus of fibrosis within the pancreas	—	—	1/6	—	—	—	—	—	—	—
Reproductive organs										
Multifocal testicular degeneration	1/5	N/A	—	N/A	—	N/A	—	N/A	—	N/A
Unilaterally, the epididymis is filled with viable and degenerate neutrophils	—	—	1/6	N/A	—	N/A	—	N/A	—	N/A
Mild uterine dilation	N/A	—	N/A	—	N/A	—	N/A	—	N/A	1/5

(—): not observed in any animals; N/A: not applicable.

conjunctivitis and corneal opacification[66]. In this study, we found that corneal clouding was independent of treatment. It occurred in sham, vehicle and treatment groups and was most often associated with prolapsed eyelashes and cage bedding embedded beneath the eyelid. Unfortunately, corneal opacification prevented *in vivo* clinical evaluation beyond 3 months of follow-up. In addition to the corneal clouding disadvantage, the RNU rat has a normal retina and as such is not useful for evaluating treatment efficacy.

For studies designed to evaluate treatment efficacy, immunocompromised retinal degenerative rats would be ideal. To that end, in 2014 Seiler and colleagues[46] reported production of an immunocompromised rat model of retinitis pigmentosa that was generated by crossing the RNU rat with the retinal degenerative rhodopsin s334ter rat[67] allowing the transplantation of human embryonic stem cell–derived neural progenitor cells that survived in its subretinal space for more that 180 days following transplant[67]. In 2018, Thomas and colleagues reported production of a similar model by crossing the RNU rat with the Royal College of Surgeons (RCS) Mertk mutant rat[68], which also accepted human subretinal xenografts without immune rejection[68]. However, the lack of commercial availability of these animals precluded their use for this large toxicity study.

Among the remaining translational challenges for the development of photoreceptor cell replacement therapy is the study of factors affecting cell survival and synaptic integration. Because these factors involve delicate interactions between the transplanted cells and host retina, these experiments are best carried out *in vivo* using animal models of retinal degeneration. Although immune suppressed backgrounds that support xenografts may be suitable for this purpose, an alternative approach would be to develop strain specific rat iPSC lines[69–72] that could be transplanted as autologous grafts in the absence of immunosuppression. However, there is no guarantee that results derived from such animal models would directly translate to adult humans. Thus, the field will need to weigh the potential risk of initiating human clinical trials with imperfect efficacy data against the potential benefits that would be afforded should blind patients regain some useful vision. We believe that the favorable safety profile presented here provides compelling support for initiating a human clinical safety trial in patients with advanced disease and very poor vision. Such safety trials could be performed in parallel with continued *in vitro* and animal research focused on enhancing graft axon extension and promoting host-donor synaptic integration.

Ethical Approval

Approval to obtain dermal fibroblast cells and generate iPSCs from patients with inherited retinal degeneration and normal controls was obtained under informed consent. This study was reviewed and approved by the University of Iowa Institutional Review Board (IRB# 200202022).

Statement of Human and Animal Rights

All procedures in this study were conducted in accordance with the University of Iowa's Institutional Review Board (IRB# 200202022), the University of Iowa's Animal Care and Use Committee (animal welfare assurance #8051317) and the ARVO statement for the use of animals in ophthalmic and vision research.

Statement of Informed Consent

Written informed consent was obtained from the patient(s) for their anonymized information to be published in this article (IRB# 200202022).

Declaration of Conflicting Interests

The author(s) declared no potential conflicts of interest with respect to the research, authorship, and/or publication of this article.

Funding

The author(s) disclosed receipt of the following financial support for the research, authorship, and/or publication of this article: This work was supported by the University of Iowa Institute for Vision Research, University of Iowa, Iowa City, IA, USA; the Elmer and Sylvia Sramek Charitable Trust, Research to Prevent Blindness; and National Institutes of Health Grant (NIH; Bethesda, MD, USA): R01 EY 024605 and P30 EY025580.

ORCID iD

Budd A. Tucker https://orcid.org/0000-0003-2178-1742

References

1. Grigoryan EN, Markitantova YV. Cellular and molecular preconditions for retinal pigment epithelium (RPE) natural reprogramming during retinal regeneration in Urodela. Biomedicines. 2016;4(4):28.
2. Tucker BA, Park IH, Qi SD, Klassen HJ, Jiang C, Yao J, Redenti S, Daley GQ, Young MJ. Transplantation of adult mouse iPS cell-derived photoreceptor precursors restores retinal structure and function in degenerative mice. PLoS ONE. 2011;6(4):e18992.
3. Mandai M, Fujii M, Hashiguchi T, Sunagawa GA, Ito SI, Sun J, Kaneko J, Sho J, Yamada C, Takahashi M. IPSC-derived retina transplants improve vision in rd1 end-stage retinal-degeneration mice. Stem Cell Rep. 2017;8(4):1112–13.
4. Singh MS, Charbel Issa P, Butler R, Martin C, Lipinski DM, Sekaran S, Barnard AR, MacLaren RE. Reversal of end-stage retinal degeneration and restoration of visual function by photoreceptor transplantation. Proc Natl Acad Sci U S A. 2013;110(3):1101–106.
5. Lin B, McLelland BT, Aramant RB, Thomas BB, Nistor G, Keirstead HS, Seiler MJ. Retina organoid transplants develop photoreceptors and improve visual function in RCS rats with RPE dysfunction. Invest Ophthalmol Vis Sci. 2020;61(11):34.
6. McLelland BT, Lin B, Mathur A, Aramant RB, Thomas BB, Nistor G, Keirstead HS, Seiler MJ. Transplanted hESC-derived retina organoid sheets differentiate, integrate, and improve visual function in retinal degenerate rats. Invest Ophthalmol Vis Sci. 2018;59(6):2586–603.

7. Zerti D, Hilgen G, Dorgau B, Collin J, Ader M, Armstrong L, Sernagor E, Lako M. Transplanted pluripotent stem cell-derived photoreceptor precursors elicit conventional and unusual light responses in mice with advanced retinal degeneration. Stem Cells. 2021;39(7):882–96.
8. Santos-Ferreira T, Volkner M, Borsch O, Haas J, Cimalla P, Vasudevan P, Carmeliet P, Corbeil D, Michalakis S, Koch E, Karl MO, et al. Stem cell-derived photoreceptor transplants differentially integrate into mouse models of cone-rod dystrophy. Invest Ophthalmol Vis Sci. 2016;57(7):3509–20.
9. Gagliardi G, Ben M'Barek K, Chaffiol A, Slembrouck-Brec A, Conart JB, Nanteau C, Rabesandratana O, Sahel JA, Duebel J, Orieux G, Reichman S, et al. Characterization and transplantation of CD73-positive photoreceptors isolated from human iPSC-derived retinal organoids. Stem Cell Rep. 2018;11(3):665–80.
10. Chao JR, Lamba DA, Klesert TR, Torre A, Hoshino A, Taylor RJ, Jayabalu A, Engel AL, Khuu TH, Wang RK, Neitz M, et al. Transplantation of human embryonic stem cell-derived retinal cells into the subretinal space of a non-human primate. Transl Vis Sci Technol. 2017;6(3):4.
11. Zhu J, Cifuentes H, Reynolds J, Lamba DA. Immunosuppression via loss of IL2rγ enhances long-term functional integration of hESC-derived photoreceptors in the mouse retina. Cell Stem Cell. 2017;20(3):374–3845.
12. Lamba DA, McUsic A, Hirata RK, Wang PR, Russell D, Reh TA. Generation, purification and transplantation of photoreceptors derived from human induced pluripotent stem cells. PLoS ONE. 2010;5(1):e8763.
13. Lamba DA, Gust J, Reh TA. Transplantation of human embryonic stem cell-derived photoreceptors restores some visual function in Crx-deficient mice. Cell Stem Cell. 2009;4(1):73–79.
14. Lingam S, Liu Z, Yang B, Wong W, Parikh BH, Ong JY, Goh D, Wong DSL, Tan QSW, Tan GSW, Holder GE, et al. CGMP-grade human iPSC-derived retinal photoreceptor precursor cells rescue cone photoreceptor damage in non-human primates. Stem Cell Res Ther. 2021;12(1):464.
15. Aboualizadeh E, Phillips MJ, McGregor JE, DiLoreto DA Jr, Strazzeri JM, Dhakal KR, Bateman B, Jager LD, Nilles KL, Stuedemann SA, Ludwig AL, et al. Imaging transplanted photoreceptors in living nonhuman primates with single-cell resolution. Stem Cell Rep. 2020;15(2):482–97.
16. Kruczek K, Gonzalez-Cordero A, Goh D, Naeem A, Jonikas M, Blackford SJI, Kloc M, Duran Y, Georgiadis A, Sampson RD, Maswood RN, et al. Differentiation and transplantation of embryonic stem cell-derived cone photoreceptors into a mouse model of end-stage retinal degeneration. Stem Cell Rep. 2017;8(6):1659–74.
17. Kashani AH, Lebkowski JS, Rahhal FM, Avery RL, Salehi-Had H, Chen S, Chan C, Palejwala N, Ingram A, Dang W, Lin CM, et al. One-year follow-up in a phase 1/2a clinical trial of an allogeneic RPE cell bioengineered implant for advanced dry age-related macular degeneration. Transl Vis Sci Technol. 2021;10(10):13.
18. Li SY, Liu Y, Wang L, Wang F, Zhao TT, Li QY, Xu HW, Meng XH, Hao J, Zhou Q, Wang L, et al. A phase I clinical trial of human embryonic stem cell-derived retinal pigment epithelial cells for early-stage Stargardt macular degeneration: 5-years' follow-up. Cell Prolif. 2021;54(9):e13100.
19. Mehat MS, Sundaram V, Ripamonti C, Robson AG, Smith AJ, Borooah S, Robinson M, Rosenthal AN, Innes W, Weleber RG, Lee RWJ, et al. Transplantation of human embryonic stem cell-derived retinal pigment epithelial cells in macular degeneration. Ophthalmology. 2018;125(11):1765–75.
20. da Cruz L, Fynes K, Georgiadis O, Kerby J, Luo YH, Ahmado A, Vernon A, Daniels JT, Nommiste B, Hasan SM, Gooljar SB, et al. Phase 1 clinical study of an embryonic stem cell-derived retinal pigment epithelium patch in age-related macular degeneration. Nat Biotechnol. 2018;36(4):328–37.
21. Mandai M, Watanabe A, Kurimoto Y, Hirami Y, Morinaga C, Daimon T, Fujihara M, Akimaru H, Sakai N, Shibata Y, Terada M, et al. Autologous induced stem-cell-derived retinal cells for macular degeneration. N Engl J Med. 2017;376(11):1038–46.
22. Falkner-Radler CI, Krebs I, Glittenberg C, Povazay B, Drexler W, Graf A, Binder S. Human retinal pigment epithelium (RPE) transplantation: outcome after autologous RPE-choroid sheet and RPE cell-suspension in a randomised clinical study. Br J Ophthalmol. 2011;95(3):370–75.
23. Wong IY, Poon MW, Pang RT, Lian Q, Wong D. Promises of stem cell therapy for retinal degenerative diseases. Graefes Arch Clin Exp Ophthalmol. 2011;249(10):1439–48.
24. Ahmed I, Johnston RJ Jr, Singh MS. Pluripotent stem cell therapy for retinal diseases. Ann Transl Med. 2021;9(15):1279.
25. Eberle D, Santos-Ferreira T, Grahl S, Ader M. Subretinal transplantation of MACS purified photoreceptor precursor cells into the adult mouse retina. J Vis Exp. 2014;84:e50932.
26. Lakowski J, Han YT, Pearson RA, Gonzalez-Cordero A, West EL, Gualdoni S, Barber AC, Hubank M, Ali RR, Sowden JC. Effective transplantation of photoreceptor precursor cells selected via cell surface antigen expression. Stem Cells. 2011; 29(9):1391–404.
27. Semo M, Haamedi N, Stevanato L, Carter D, Brooke G, Young M, Coffey P, Sinden J, Patel S, Vugler A. Efficacy and safety of human retinal progenitor cells. Transl Vis Sci Technol. 2016;5(4):6.
28. Luo J, Baranov P, Patel S, Ouyang H, Quach J, Wu F, Qiu A, Luo H, Hicks C, Zeng J, Zhu J, et al. Human retinal progenitor cell transplantation preserves vision. J Biol Chem. 2014; 289(10):6362–71.
29. Aftab U, Jiang C, Tucker B, Kim JY, Klassen H, Miljan E, Sinden J, Young M. Growth kinetics and transplantation of human retinal progenitor cells. Exp Eye Res. 2009;89(3):301–10.
30. Ballios BG, Cooke MJ, Donaldson L, Coles BL, Morshead CM, van der Kooy D, Shoichet MS. A hyaluronan-based injectable hydrogel improves the survival and integration of stem cell progeny following transplantation. Stem Cell Rep. 2015;4(6):1031–45.
31. Barber AC, Hippert C, Duran Y, West EL, Bainbridge JW, Warre-Cornish K, Luhmann UF, Lakowski J, Sowden JC, Ali RR, Pearson RA. Repair of the degenerate retina by photoreceptor transplantation. Proc Natl Acad Sci U S A. 2013;110(1):354–59.
32. Klassen H, Sakaguchi DS, Young MJ. Stem cells and retinal repair. Prog Retin Eye Res. 2004;23(2):149–81.
33. MacLaren RE, Pearson RA, MacNeil A, Douglas RH, Salt TE, Akimoto M, Swaroop A, Sowden JC, Ali RR. Retinal repair by transplantation of photoreceptor precursors. Nature. 2006;444(7116):203–207.

34. Redenti S, Neeley WL, Rompani S, Saigal S, Yang J, Klassen H, Langer R, Young MJ. Engineering retinal progenitor cell and scrollable poly(glycerol-sebacate) composites for expansion and subretinal transplantation. Biomaterials. 2009;30(20):3405–14.
35. Tomita M, Lavik E, Klassen H, Zahir T, Langer R, Young MJ. Biodegradable polymer composite grafts promote the survival and differentiation of retinal progenitor cells. Stem Cells. 2005;23(10):1579–88.
36. Tucker BA, Redenti SM, Jiang C, Swift JS, Klassen HJ, Smith ME, Wnek GE, Young MJ. The use of progenitor cell/biodegradable MMP2-PLGA polymer constructs to enhance cellular integration and retinal repopulation. Biomaterials. 2010;31(1):9–19.
37. Thompson JR, Worthington KS, Green BJ, Mullin NK, Jiao C, Kaalberg EE, Wiley LA, Han IC, Russell SR, Sohn EH, Guymon CA, et al. Two-photon polymerized poly(caprolactone) retinal cell delivery scaffolds and their systemic and retinal biocompatibility. Acta Biomater. 2019;94:204–18.
38. Worthington KS, Wiley LA, Kaalberg EE, Collins MM, Mullins RF, Stone EM, Tucker BA. Two-photon polymerization for production of human iPSC-derived retinal cell grafts. Acta Biomater. 2017;55:385–95.
39. Sharma R, Khristov V, Rising A, Jha BS, Dejene R, Hotaling N, Li Y, Stoddard J, Stankewicz C, Wan Q, Zhang C, et al. Clinical-grade stem cell-derived retinal pigment epithelium patch rescues retinal degeneration in rodents and pigs. Sci Transl Med. 2019;11(475):eaat5580.
40. Pennington BO, Clegg DO, Melkoumian ZK, Hikita ST. Defined culture of human embryonic stem cells and xeno-free derivation of retinal pigmented epithelial cells on a novel, synthetic substrate. Stem Cells Transl Med. 2015;4(2):165–77.
41. Lee IK, Ludwig AL, Phillips MJ, Lee J, Xie R, Sajdak BS, Jager LD, Gong S, Gamm DM, Ma Z. Ultrathin micromolded 3D scaffolds for high-density photoreceptor layer reconstruction. Sci Adv. 2021;7(17):eabf0344.
42. Jung YH, Phillips MJ, Lee J, Xie R, Ludwig AL, Chen G, Zheng Q, Kim TJ, Zhang H, Barney P, Min J, et al. 3D microstructured scaffolds to support photoreceptor polarization and maturation. Adv Mater. 2018;30(39):e1803550.
43. Douglas-Jones A, Nelson J, Jansen V, Miller T. Characterization of the (rnunz) nude rat. Morphological characteristics of the lymphoid system. Aust J Exp Biol Med Sci. 1981;59(pt 3):277–86.
44. Terada E, Nakayama T, Hioki K, Saito M, Okudaira H. [Absence of T lymphocyte functions in athymic nude rats (author's transl)]. Jikken Dobutsu. 1980;29(3):365–67.
45. Salinas-Carmona MC, Nussenblatt RB, Gery I. Experimental autoimmune uveitis in the athymic nude rat. Eur J Immunol. 1982;12(6):480–84.
46. Seiler MJ, Aramant RB, Jones MK, Ferguson DL, Bryda EC, Keirstead HS. A new immunodeficient pigmented retinal degenerate rat strain to study transplantation of human cells without immunosuppression. Graefes Arch Clin Exp Ophthalmol. 2014;252(7):1079–92.
47. Khristov V, Maminishkis A, Amaral J, Rising A, Bharti K, Miller S. Validation of iPS cell-derived RPE tissue in animal models. Adv Exp Med Biol. 2018;1074:633–40.
48. Wiley LA, Burnight ER, DeLuca AP, Anfinson KR, Cranston CM, Kaalberg EE, Penticoff JA, Affatigato LM, Mullins RF, Stone EM, Tucker BA. cGMP production of patient-specific iPSCs and photoreceptor precursor cells to treat retinal degenerative blindness. Sci Rep. 2016;6:30742.
49. Bohrer LR, Wiley LA, Burnight ER, Cooke JA, Giacalone JC, Anfinson KR, Andorf JL, Mullins RF, Stone EM, Tucker BA. Correction of NR2E3 associated enhanced S-cone syndrome patient-specific iPSCs using CRISPR-Cas9. Genes (Basel). 2019;10(4):278.
50. Light JG, Fransen JW, Adekunle AN, Adkins A, Pangeni G, Loudin J, Mathieson K, Palanker DV, McCall MA, Pardue MT. Inner retinal preservation in rat models of retinal degeneration implanted with subretinal photovoltaic arrays. Exp Eye Res. 2014;128:34–42.
51. Lorach H, Kang S, Bhuckory MB, Trouillet A, Dalal R, Marmor M, Palanker D. Transplantation of mature photoreceptors in rodents with retinal degeneration. Transl Vis Sci Technol. 2019;8(3):30.
52. Wiley LA, Anfinson KR, Cranston CM, Kaalberg EE, Collins MM, Mullins RF, Stone EM, Tucker BA. Generation of xeno-free, cGMP-compliant patient-specific iPSCs from skin biopsy. Curr Protoc Stem Cell Biol. 2017;42:4A.12.1–14.
53. Fligor CM, Lavekar SS, Harkin J, Shields PK, VanderWall KB, Huang KC, Gomes C, Meyer JS. Extension of retinofugal projections in an assembled model of human pluripotent stem cell-derived organoids. Stem Cell Rep. 2021;16(9):2228–41.
54. Fligor CM, Huang KC, Lavekar SS, VanderWall KB, Meyer JS. Differentiation of retinal organoids from human pluripotent stem cells. Methods Cell Biol. 2020;159:279–302.
55. Zhong X, Gutierrez C, Xue T, Hampton C, Vergara MN, Cao LH, Peters A, Park TS, Zambidis ET, Meyer JS, Gamm DM, et al. Generation of three-dimensional retinal tissue with functional photoreceptors from human iPSCs. Nat Commun. 2014;5:4047.
56. Kallman A, Capowski EE, Wang J, Kaushik AM, Jansen AD, Edwards KL, Chen L, Berlinicke CA, Joseph Phillips M, Pierce EA, Qian J, et al. Investigating cone photoreceptor development using patient-derived NRL null retinal organoids. Commun Biol. 2020;3(1):82.
57. Capowski EE, Samimi K, Mayerl SJ, Phillips MJ, Pinilla I, Howden SE, Saha J, Jansen AD, Edwards KL, Jager LD, Barlow K, et al. Reproducibility and staging of 3D human retinal organoids across multiple pluripotent stem cell lines. Development. 2019;146(1):dev171686.
58. Cuevas E, Holder DL, Alshehri AH, Treguier J, Lakowski J, Sowden JC. NRL(-/-) gene edited human embryonic stem cells generate rod-deficient retinal organoids enriched in S-cone-like photoreceptors. Stem Cells. 2021;39(4):414–28.
59. Lakowski J, Welby E, Budinger D, Di Marco F, Di Foggia V, Bainbridge JWB, Wallace K, Gamm DM, Ali RR, Sowden JC. Isolation of human photoreceptor precursors via a cell surface marker panel from stem cell-derived retinal organoids and fetal retinae. Stem Cells. 2018;36(5):709–22.
60. Jha BS, Farnoodian M, Bharti K. Regulatory considerations for developing a phase I investigational new drug application for autologous induced pluripotent stem cells-based therapy product. Stem Cells Transl Med. 2021;10(2):198–208.
61. Krivosic V, Kamami-Levy C, Jacob J, Richard S, Tadayoni R, Gaudric A. Laser photocoagulation for peripheral retinal capillary hemangioblastoma in von Hippel-Lindau disease. Ophthalmol Retina. 2017;1(1):59–67.

62. Bowen RC, Boldt HC, Mullins RF, Field MG, Affatigato LM, Hoffmann JM, Folk JC, Gehrs KM, Han IC, Sohn EH, Russell SR, et al. Intrafamilial variability of ocular manifestations of von Hippel-Lindau disease. Ophthalmol Retina. 2021;6:89–91.
63. Thackaberry EA, Farman C, Zhong F, Lorget F, Staflin K, Cercillieux A, Miller PE, Schuetz C, Chang D, Famili A, Daugherty AL, et al. Evaluation of the toxicity of intravitreally injected PLGA microspheres and rods in monkeys and rabbits: effects of depot size on inflammatory response. Invest Ophthalmol Vis Sci. 2017;58(10):4274–85.
64. Thompson JR, Worthington KS, Green BJ, Mullin NK, Jiao C, Kaalberg EE, Wiley LA, Han IC, Russell SR, Sohn EH, Guymon CA, et al. Two-photon polymerized poly(caprolactone) retinal cell delivery scaffolds and their systemic and retinal biocompatibility. Acta Biomater. 2019;94:204–18.
65. Tucker BA, Mullins RF, Streb LM, Anfinson K, Eyestone ME, Kaalberg E, Riker MJ, Drack AV, Braun TA, Stone EM. Patient-specific iPSC-derived photoreceptor precursor cells as a means to investigate retinitis pigmentosa. Elife. 2013;2:e00824.
66. Pardue MT, Phillips MJ, Yin H, Sippy BD, Webb-Wood S, Chow AY, Ball SL. Neuroprotective effect of subretinal implants in the RCS rat. Invest Ophthalmol Vis Sci. 2005;46(2):674–82.
67. Moore GJ. Conjunctivitis in the nude rat (rnu/rnu). Lab Anim. 1979;13(1):35.
68. Bryda EC, LaVail MM. Letter to the editor announcing the availability of RCS and transgenic rats with P23H and S334ter rhodopsin mutations with inherited retinal degenerations. Exp Eye Res. 2019;178:176.
69. Thomas BB, Zhu D, Lin TC, Kim YC, Seiler MJ, Martinez-Camarillo JC, Lin B, Shad Y, Hinton DR, Humayun MS. A new immunodeficient retinal dystrophic rat model for transplantation studies using human-derived cells. Graefes Arch Clin Exp Ophthalmol. 2018;256(11):2113–25.
70. Yamaguchi T, Hamanaka S, Nakauchi H. The generation and maintenance of rat induced pluripotent stem cells. Methods Mol Biol. 2014;1210:143–50.
71. Hamanaka S, Yamaguchi T, Kobayashi T, Kato-Itoh M, Yamazaki S, Sato H, Umino A, Wakiyama Y, Arai M, Sanbo M, Hirabayashi M, et al. Generation of germline-competent rat induced pluripotent stem cells. PLoS ONE. 2011;6(7):e22008.
72. Liao J, Cui C, Chen S, Ren J, Chen J, Gao Y, Li H, Jia N, Cheng L, Xiao H, Xiao L. Generation of induced pluripotent stem cell lines from adult rat cells. Cell Stem Cell. 2009;4(1):11–15.